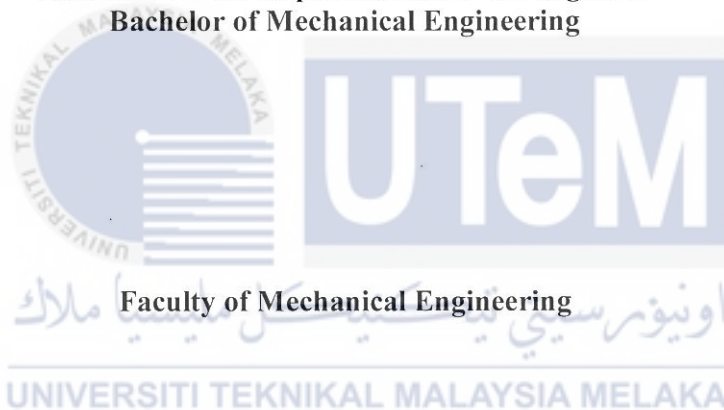


CFD STUDY OF AN OSCILLATORY FLOW ACROSS HEAT EXCHANGER

EDZZRY INDRAWAN BIN FAIZAL EDZUAN

A report submitted
fulfillment of the requirements for the degree of
Bachelor of Mechanical Engineering



UNIVERSITI TEKNIKAL MALAYSIA MELAKA

2020

DECLARATION

I declare that this project entitled “CFD study of an oscillatory flow across heat exchanger” is the result of my own work except as cited in the references.

 Signature : 

Name : EDZRY INDRAWAN BIN FAIZAL EDZUAN

 Date : 17-7-2020

UNIVERSITI TEKNIKAL MALAYSIA MELAKA

DEDICATION

I dedicate this project report to my loved family members who have support me and showed unending support. They have helped me in making this project a success. I would also dedicate this project report to the field of research. The contents within this project report should be helpful for future researches and studies.



ABSTRACT

This study focuses on the study of oscillatory flow at various drive ratios across a heat exchanger by using CFD modelling. The primary goal of a heat exchanger is to exchange heat between two fluids, hence the performance of the heat exchanger in terms of heat transfer is significant. Fluid flow can be of either steady flow, where fluid exits the system after heat is exchanged, or of oscillatory flow, where the fluid stays in the system oscillating back and forth periodically in a heat exchanger. The geometry model for the heat exchanger was modelled using Ansys Design Modeler. Grid independency test was conducted to determine the appropriate grid size to be used when solving the model. Four models of oscillatory flow of different DR were solved using Ansys Fluent. The results obtained was compared with theoretical calculations to determine the validity. Several contour plots of velocity, vorticity, temperature, and pressure were plotted. Heat transfer performance was analyzed by obtaining the surface heat transfer coefficient at the tubes and thus obtaining the heat transfer rates. Higher drive ratio, DR, provides greater heat transfer within the heat exchanger and the tube banks due to the turbulence generation. Since oscillatory flow has yet to have conclusive equations to model the heat transfer, steady flow heat transfer equations are used.

UNIVERSITI TEKNIKAL MALAYSIA MELAKA

ABSTRAK

Kajian ini memberi fokus terhadap ujikaji aliran berayun merentasi penukar haba pada nisbah pemacu yang berbeza dengan menggunakan kaedah pemodelan dinamik aliran bendalir. Matlamat utama penukar haba adalah untuk memindahkan haba di antara dua bendalir. Oleh itu, prestasi penukar haba dari segi pemindahan haba adalah penting. Aliran bendalir boleh diklasifikasikan dalam dua bentuk iaitu aliran stabil, di mana bendalir keluar daripada sistem setelah pertukaran haba, atau aliran berayun, di mana bendalir berada di dalam sistem sambil berayun ulang-alik secara berkala di dalam penukar haba. Model geometri penukar haba telah dimodelkan menggunakan Ansys Design Modeler. Ujian kebebasan grid telah dilakukan untuk menentukan ukuran grid yang sesuai dalam menyelesaikan model. Empat model aliran berayun pada nisbah pemacu yang berbeza telah diselesaikan menggunakan Ansys Fluent. Hasil yang diperolehi telah dibandingkan dengan pengiraan teori untuk menentukankan kesahihan. Beberapa plot kontur halaju, vortisiti, suhu, dan tekanan telah diplot. Prestasi penukar haba telah dianalisis dengan mendapatkan pekali pemindahan haba permukaan pada tiub dan mendapatkan kadar pemindahan haba. Nisbah pemacu yang lebih tinggi memberikan pemindahan haba yang lebih besar diantara penukar haba dan susunan tiub oleh sebab pergolakan yg dihasilkan. Disebabkan aliran berayun belum mempunyai persamaan yang boleh memodelkan pemindahan haba dengan tepat, persamaan pemindahan haba untuk aliran stabil telah digunakan.

ACKNOWLEDGEMENT

Firstly, I would like to give my appreciation to my supervisor, Dr. Fatimah Al-Zahrah binti Mohd Sa'at for her dedicated guidance and assistance during this study. Her wide vast knowledge and experience specifically in this study field has helped me further my understanding in the study, perform research correctly, and expressing findings clearly in the report. Without her guidance and moral supports throughout the year, my completion of this study might not been able to be accomplished.

Besides my supervisor, I would also like to thank Dr. Fadhilah binti Shikh Anuar and En. Mohd Noor Asril as my second reviewer and second seminar panel. Their positive comments, opinion, and suggestions about my study has helped to improve the contents of my final report.

Futhermore, my utmost gratitude is given to the faculty for giving me the opportunity to perform my final year project. Special appreciation to the chairman of the final year project committee, Dr. Fadhli bin Syahrial for the clear instructions and steps to provide a proper final year project report according to the guideline specified.

I would also like to thank my family members for giving me the opportunity to further my study, their unwavering support, and words of encouragement throughout my study.

CONTENT

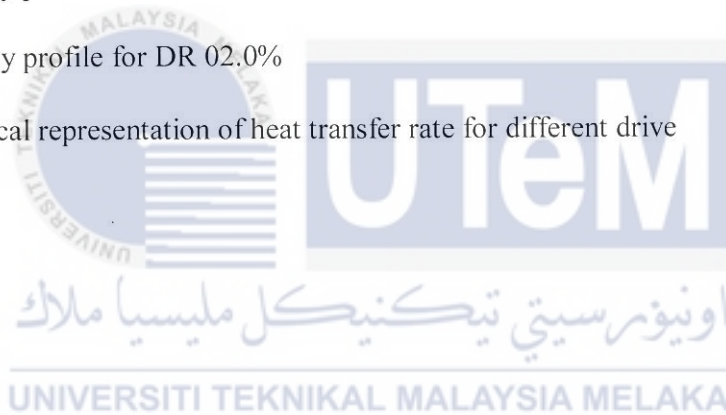
CHAPTER	CONTENT	PAGE
	DECLARATION	
	APPROVAL	
	DEDICATION	
	ABSTRACT	i
	ABSTRAK	ii
	ACKNOWLEDGEMENT	iii
	TABLE OF CONTENT	iv-v
	LIST OF FIGURES	vi-vii
	LIST OF TABLES	viii-ix
	LIST OF ABBREVIATIONS	x
	LIST OF SYMBOLS	xi
CHAPTER 1	INTRODUCTION	1
	1.1 Background	1-2
	1.2 Problem Statement	2
	1.3 Objectives	2
	1.4 Scope of Project	4
CHAPTER 2	LITERATURE REVIEW	5
	2.1 Types of flow	5
	2.1.1 Internal flow	5
	2.1.2 External Flow	6
	2.1.3 Steady flow vs unsteady flow	6
	2.1.4 Cross flow	6-7
	2.1.5 Oscillatory flow	7-8
	2.2 Flow over tube banks	9
	2.2.1 Boundary layer	9-10
	2.2.2 No-slip condition	10-11

2.2.3	Stagnation	11
2.2.4	Flow separation	11-12
2.2.5	Reynolds number	12
2.3	Heat transfer performance for oscillatory flow	12-13
2.3.1	Convection	13-14
2.3.2	Nusselt number	14-16
2.3.3	Prandtl number	16
2.3.4	Experimental research on oscillatory flow	16-17
2.3.5	CFD research on oscillatory flow	17-18
CHAPTER 3	METHODOLOGY	19
3.1	Project planning flowchart	19-20
3.2	Developing CFD model	21
3.3	Defining geometry and flow domain	22
3.4	Selection of discretization model and mesh setup	22-25
3.5	Setting up of oscillatory flow model	25-27
3.6	Solving and visualizing of oscillatory model	28-29
3.7	Grid test	29
3.7.1	Mesh quality	29-30
3.7.2	Grid independency test	30-31
3.7.3	Grid selection	31-32
CHAPTER 4	RESULT AND DISCUSSION	33
4.1	Validation of oscillatory flows	33-35
4.2	Velocity contour	35-39
4.3	Vorticity Contour	39-41
4.4	Temperature Contour	42-43
4.5	Pressure Contour	44-45
4.6	Heat transfer coefficient	46-47
CHAPTER 5	CONCLUSION AND RECOMMENDATIONS	48
	REFERENCE	49-52
	APPENDICES	53-61

LIST OF FIGURES

FIGURE	TITLE	PAGE
2.1	Illustration of internal flow.	6
2.2	Illustration of cross flow	7
2.3	Velocity profiles of oscillatory flow at different Womersly number	8
2.4	Development of boundary layer for different flow regimes	9
2.5	Changing of velocity profile due to no-slip condition	10
2.6	Flow separation and wake region	11
2.7	Local Nusselt number around cylinder subjected to cross flow of air	15
3.1	Research methodology flowchart	20
3.2	Sketch of 2D staggered tube bank model	21
3.3	Named selections for surface model of tube banks	22
3.4	Overall Meshing	24
3.5	Enlarged view of mesh around the tube walls.	24
3.6	Edge sizing	25

3.7	Graph for oscillating velocity at DR 1.2%	30
3.8	Graph for oscillating pressure at DR 1.2%	31
4.1	Graph comparison of oscillation velocity at DR 0.83%	33
4.2	Graph comparison of oscillation velocity at DR 1.2%	34
4.3	Graph comparison of oscillation velocity at DR 1.5%	34
4.4	Graph comparison of oscillation velocity at DR 2.0%	35
4.5	Velocity profile for DR 0.83%	36
4.6	Velocity profile for DR 1.5%	36
4.7	Velocity profile for DR 1.5%	37
4.8	Velocity profile for DR 02.0%	37
4.9	Graphical representation of heat transfer rate for different drive ratios.	47



LIST OF TABLES

TABLE	TITLE	PAGE
3.1	Dimensions of the tube banks	21
3.2	Details of mesh sizing option	23
3.3	Boundary conditions	26
3.4.	Fluid properties	27
3.5	Mesh quality of grids	30
3.6	Range of skewness and cell quality	32
4.1	Velocity contour for drive ratio 0.83% and 1.2%	38
4.2	Velocity contour for drive ratio 1.5% and 2.0%	39
4.3	Vorticity contour for drive ratio 0.83% and 1.2%	40
4.4	Vorticity contour for drive ratio 1.5% and 2.0%	41
4.5	Temperature contour for drive ratio 0.83% and 1.2%	42
4.6	Temperature contour for drive ratio 1.5% and 2.0%	43
4.7	Pressure contour for drive ratio 0.83% and 1.2%	44
4.8	Pressure contour for drive ratio 1.5% and 2.0%	45

4.9	Surface heat transfer coefficient	46
4.10	Calculated heat transfer rate	47



LIST OF ABBEREVATIONS

CFD	Computational Fluid Dynamics
HWA	Hot-wire Anemometry
DR	Drive Ratio
PISO	Pressure-Implicit Splitting Operators



LIST OF SYMBOL

α	=	Womersly number
L_C	=	Characteristic length
μ	=	Dynamic viscosity
ρ	=	Density
ω	=	Angular frequency
Re	=	Reynolds number
V	=	Velocity
ν	=	Kinematic viscosity
h	=	Convection heat transfer coefficient
\dot{Q}	=	Rate of heat convection
A	=	Area of heat transfer
T_{LMTD}	=	Log mean temperature difference
ΔT_i	=	Temperature difference at the inlet
ΔT_e	=	Temperature difference at the outlet
Nu	=	Nusselt number
k	=	Thermal conductivity
Pr	=	Prandtl number
C_p	=	Specific heat

CHAPTER 1

INTRODUCTION

1.1 Background

Heat exchangers are devices that allow the transfer of thermal energy between two or more fluids of different temperatures. Cengel and Boles (2015) defined heat exchangers as a device where two moving fluids exchange heat without mixing. Both heating and cooling processes involve the use of heat exchangers. Heat exchangers are commonly used in applications where heating and cooling of a fluid stream of concern and evaporation or condensation of single- or multicomponent fluid streams (Shah & Sekulic, 2003). Other uses of heat exchangers can be seen in room heating, refrigeration, air-conditioning etc. Heat exchangers mainly work on the basic principle of convection (in each fluid) and conduction (between the thin walls and the fluid). Therefore, selection of proper heat exchangers is vital due to various factors that influence heat transfer rates depending on need of different applications.

There are several ways to classify heat exchangers which include differentiating them by their flow configuration, construction method, or the method at which they transfer heat. In this study, crossflow heat exchanger is the main focus. Crossflow heat exchangers are defined by the flow of fluid that is perpendicular to one another. This type of heat exchanger is further classified into two different classifications, namely mixed and unmixed flow. The differences between mixed and unmixed flow is that in mixed flow, the fluid is free to move in the

transverse direction while in unmixed flow, the presence of fins only allows the fluid to move in the direction of the flow itself (Spakovszky, 2019).

In heat exchangers, tube banks are the most common type of configuration when it comes to transferring heat. The arrangements of the tube banks are usually either in-line or staggered with respect to the direction of flow. These tube banks are further classified based on their crosswise and streamwise pitch-to-diameter ratio, wherein having a ratio smaller than 1.25^2 are referred to as compact, while having a ratio larger than 4 are considered to be widely-spaced (Beale, 2011). In the case of internal flow in the tube banks, heat transfer analysis can be calculated by analysing a single tube, and multiplying the results by the amount of tubes present. However, for the case of external flow over tube banks, the tubes will affect the flow pattern and turbulence across the pipe, therefore affecting heat transfer to and from the pipes.

Heat exchanger that operates under oscillatory flow is a crucial component of thermoacoustic engines and coolers (Ilori, Jaworski, & Mao, 2018). The oscillating flow in thermoacoustic systems allows the transfer of energy within its internal component to produce acoustic power (engine) or to pump heat (cooler). Therefore, it is necessary to design an optimum heat exchanger to have thermoacoustic engines with high performance.

In this project, oscillatory flow over tube banks will be studied with the aid of Computational Fluid Dynamics (CFD) software such as ANSYS Fluent. The use of CFD will allow for easier analysis of the oscillatory flow with the help of computer simulation. It also eliminates the need for experimenting without compromising the accuracy of the results.

1.2 Problem statement

There are many different types of flows across tube banks. The general focus in this study is the oscillatory flow of fluid motion across tube banks. Fluid in an oscillatory flow moves in a manner in which it changes direction over time (including reverse motion). Some observations on oscillatory flow can be seen in situations such as water flow in oceans, blood circulation flow, and thermoacoustic engine.

There are many case studies as well as established researches that have been done towards heat transfer and fluid dynamics of fluid across tube banks especially in the case on steady one-directional flow. However, there are limited studies and literatures regarding oscillatory motion of fluid on the same subject. Therefore, in this project, the oscillatory flow of fluid across tube banks will be studied, simulated and recorded.

1.3 Objective

The objective of this project is:

1. To use CFD to model cross flow over tube banks.
2. To analyse fluid flow characteristics of oscillatory cross flow.
3. To analyse heat transfer characteristics of oscillatory cross flow.

1.4 Scope of study

The scopes of this study are:

1. Limited to the use of CFD only.
2. Only using two dimensional (2D) models.
3. Focuses on oscillatory flow only.
4. Use of circular tubes as heat exchanger.



CHAPTER 2

LITERATURE REVIEW

In this chapter, detail discussion on the information and research that had been done on the topic which is “CFD study of and oscillatory flow across heat exchangers”. Some of the related terminology will be discussed in this section which includes flow characteristics, flows over heat exchangers, performance of heat exchangers, etc.

2.1 Types of flow

In this section of the report, the types of flows that are present will be defined and explained further in detail.

2.1.1 Internal flow

Internal flow is a fluid that flows through confining walls where the flow is guided from a defined inlet and exits an outlet (Johnston, 1976). Cengel and Cimbala (2017) defined internal flow if the fluid is bounded by solid surfaces. Fluid that flows in a duct where the liquid is partially filling the duct and there is a free surface that is classified as open-channel flow. Examples of this type of flow are fluid flow through a pipe, duct, or channel. An example of this type of flow can be seen by flow of water in pipes.

2.1.2 External flow

External flow is defined as the motion of fluid around a body which is immersed in the fluid medium (Polezhaev, 2011). Examples of external flow are flow of air around an aerofoil, and flow of air around a moving car. Figure 2.1 shows an illustration of external flow.

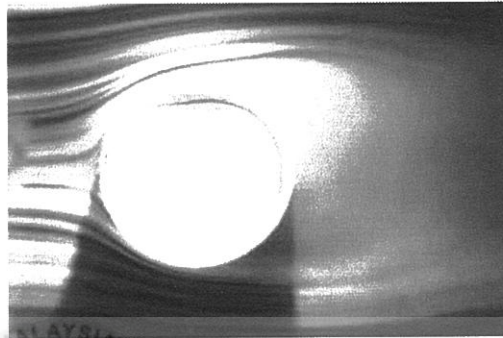


Figure 2.1: Illustration of external flow (Cengel & Cimbala, 2017)

2.1.3 Steady flow vs unsteady flow

The flow of fluid can be classified into two different flow conditions, namely steady flow and unsteady flow. Steady flow is the condition of flow when the fluid properties at any point in the system exhibits no change with respect to time. These fluid properties include temperature, density, pressure, velocity and etc. Unsteady flow or non-steady flow is a flow condition where the fluid properties of the system depend on time.

2.1.4 Cross flow

Cross flow is the type of flow where one fluid flows through pipes or tubes while the other fluid flows across the tubes in a perpendicular direction (Yoo, Kwon, & Kim, 2007). These types of heat exchangers usually operate for heat transfer between a liquid and a gas

(Bengtson, 2019). Examples of the application of cross flow heat exchanger configuration can be seen in car radiators and evaporator coil for air conditioning units. Figure 2.2 illustrates the cross flow situation.

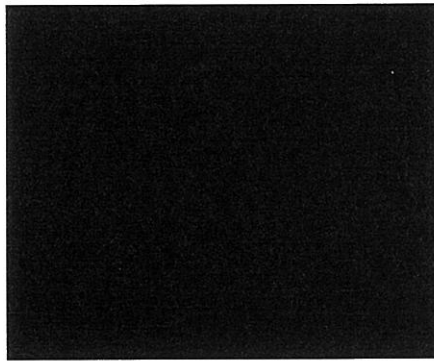


Figure 2.2: Illustration of cross flow

2.1.5 Oscillatory Flow

Oscillation can be defined as the forward and backward motion of a thing between two locations or points. This motion can be periodic which means it repeats itself in a steady cycle. Hence, oscillatory flow can be defined as a flow of a fluid moving back and forth in a regular cycle between two positions. Two forms of oscillatory flow have been studied. The first type is unidirectional oscillation about a mean pulsating flow which consists of two components; the steady and unsteady components. An example of this type of flow is the flow of blood in the arteries. The second type of oscillatory flow is reciprocating flows, which fully changes direction in the reverse direction cyclically with zero mean velocity (Jalil, 2019). There are various advantages to understanding oscillatory flows. Other examples of oscillatory flows are oscillation of the working fluid in thermoacoustics engines, and waves under the ocean.

In oscillatory flow, the velocity shape profile is dictated by the Womersley number. Womersley number, Wo , is a dimensionless parameter used most commonly in biofluid

mechanics and biofluid dynamics. It is named after John R. Womersley (1907 – 1958) for his contributions towards blood flow in arteries. The Womersley number is usually denoted by α and is represented in Eq. (1).

$$\alpha = L_C \sqrt{\frac{\omega \rho}{\mu}} \quad (1)$$

where α is the Womersley number, L_C is the characteristic length (m), ω is the angular frequency of oscillation (rad/s), ρ is the density of the fluid (kg/m^3), and μ is the dynamics viscosity of the fluid ($\text{N}\cdot\text{s/m}^2$). The Womersley number shows the ratio of transient inertia force to the shear force.

Feldmann and Wagner (2012) reported that the velocity profiles of oscillating flow can be in the shape of a parabola, M-profile or a flat profile with increasing frequency. Figure 2.3 shows the velocity profile at different Womersley number.

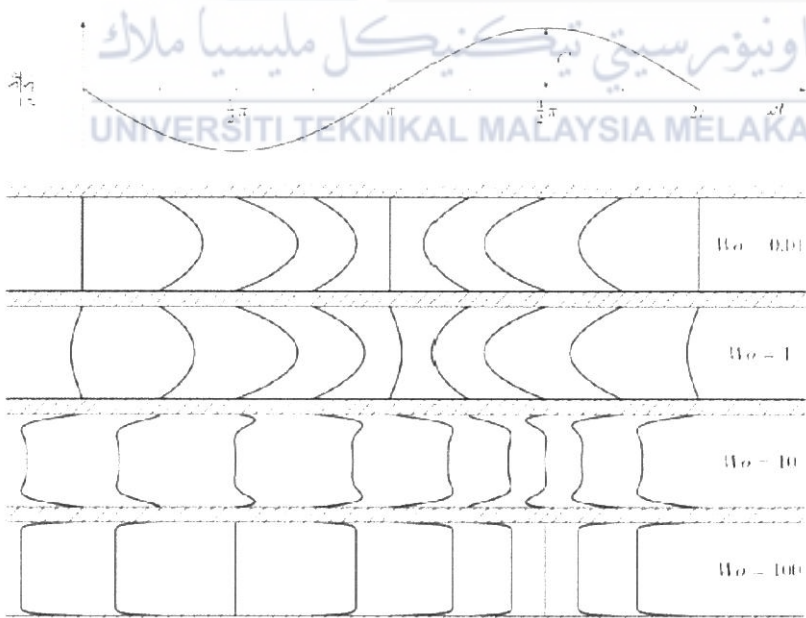


Figure 2.3: Velocity profiles of oscillatory flow at different Womersly number (Schoenmaker, 2017)

2.2 Flow over tube banks

In flow over tube banks, the fluid undergoes external flow. The tube banks act as an obstacle that obstructs the flow of the fluid. In this sub-section, the flow characteristics of the fluid in external flow will be discussed and explained such as no-slip condition, separation, stagnation and etc.

2.2.1 Boundary layer

Formation of a boundary layer begins when the first layer of the fluid flow adjacent to the surface is undergoing a no-slip condition. This motionless layer slows down the particles of the next fluid layer due to friction between the particles of the neighbouring layer. This process continues until a distance of δ from the plate beyond which the free-stream velocity remains unchanged. Figure 2.4 shows the development of boundary layer for different flow regimes.

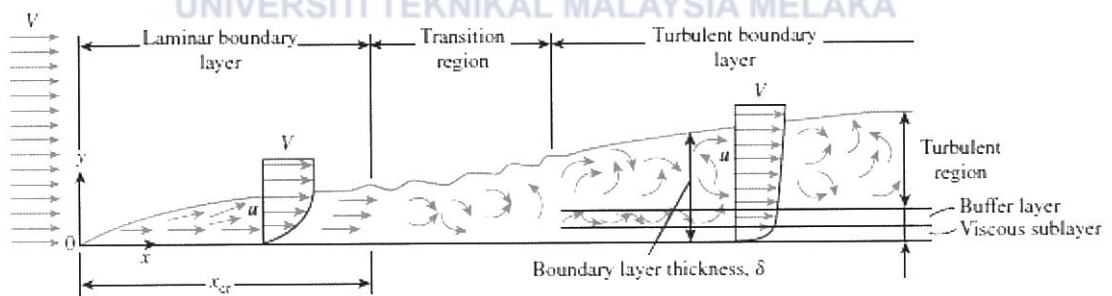


Figure 2.4: Development of boundary layer for different flow regimes (Cengel & Ghajar, 2015)

The boundary layer thickness, δ , is typically defined by distance y from the surface at $u = 0.99V$. This imaginary line of $u = 0.99V$ separates the flow into two regions: the boundary

layer region in which viscous effects are considered as well as the change in velocity, and the irrotational flow region, where frictional effects are negligible and the velocity remains constant.

2.2.1 No-slip condition

No-slip condition is a condition at which fluid is flowing over a surface of an object that have zero velocity relative to the velocity of the surface. In other words, the fluid that is moving over the surface will “stick” to the surface. However, the fluid will have velocity if the surface is moving, but the velocity of the fluid will still be zero relative to the surface of the object. Figure 2.4 shows the changing of velocity profile due to no-slip condition.

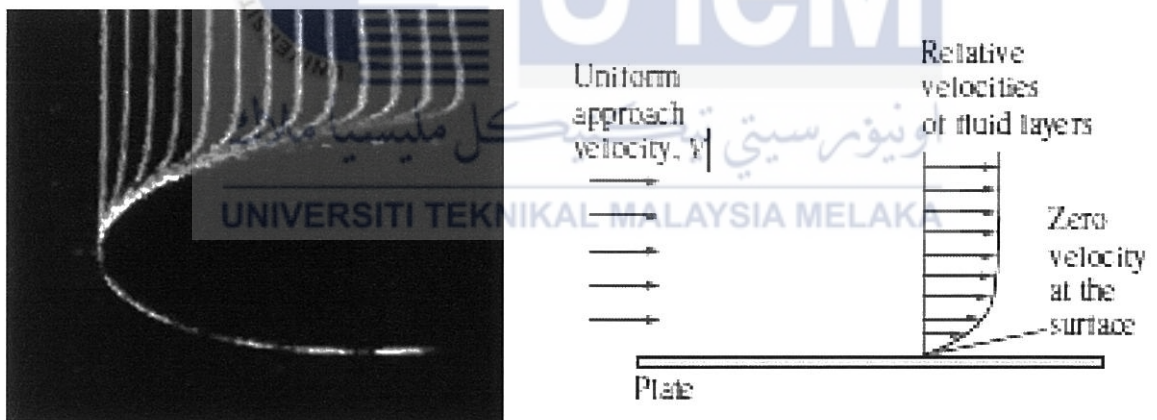


Figure 2.5: Changing of velocity profile due to no-slip condition (Cengel & Cimbala, 2017)

The layer that sticks to the surface slows down the next layer and continues to slow down the later layers due to viscous forces. Therefore, the velocity profile of a fluid is due to the no-slip condition. Prabhakara and Deshpande (2004) stated that even in turbulent flows,

which have large velocity gradients near the walls, will have to satisfy the no-slip condition at every instant.

2.2.2 Stagnation

Stagnation point is defined as the point at which local velocity of the fluid flow is equal to zero. Stagnation point form at the surface of the object in the flow field due to object that is stopping the motion of the fluid and the fluid is brought to rest.

2.2.3 Flow separation

Fluid that flows over a curved surface exhibits a phenomenon that is known as flow separation. This phenomenon occurs when the fluid flow is great enough that the fluid stream detaches itself from the surface on the back side. When the fluid separates from the body, it forms a low pressure region behind the body and is called separated region. This separated region allows for recirculating and back flow to occur. Larger separated regions will cause larger pressure drag. Separated region also affects the velocity of the flow as it slows the downstream velocity of the fluid (relative to the upstream velocity). The region of the flow that affects the velocity of the fluid is called the wake. Figure 2.5 demonstrates flow separation and wake region.

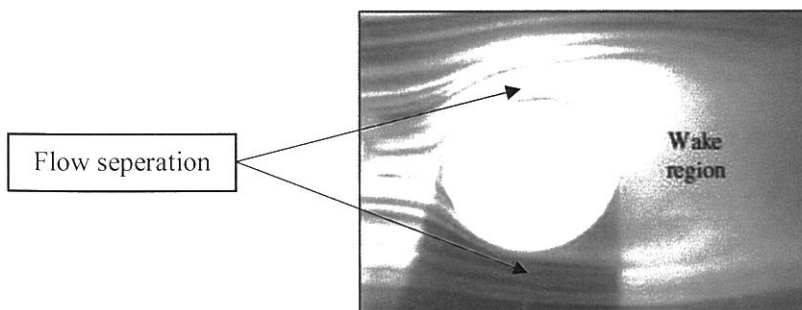


Figure 2.6: Flow separation and wake region (Cengel & Cimbala, 2017)

When the two fluid streams reattach, the separation region comes to an end. Furthermore, the wake will continue to grow in the separation region until the fluid regains its velocity. Formation and vortices are the by-products of flow separation. Vortex shedding is the continuous generation of these vortices downstream which usually occur in normal flow over long cylinders and spheres for $Re \geq 90$. These vortices that form near the body may generate vibrations near the body. If the vibration frequency is close to natural frequency of the body, the body may resonate dangerously.

2.2.4 Reynolds number

Reynolds number is a dimensionless parameter that measures the ratio of inertia forces to viscous forces in a fluid. It is named after an English engineer and physicist, Osborne Reynolds which is known for his work in the field of hydraulics and hydrodynamics. Eq. (2) expresses Reynolds number:-

$$Re = \frac{\text{Inertia forces}}{\text{Viscous forces}} = \frac{VL_c}{\nu} = \frac{\rho VL_c}{\mu} \quad (2)$$

where Re is Reynolds number, V is velocity of fluid with respect to the object (m/s), L_c is characteristic length (m), ν is the kinematic viscosity (m^2/s), ρ is the density of the fluid (kg/m^3), and μ is dynamic viscosity ($N \cdot s/m^2$).

2.3 Heat transfer performance for oscillatory flow

In steady flows across tube banks, heat transfer calculation can be done by directly applying the heat transfer correlations. However, in oscillatory flow, directly applying the heat

transfer correlations will yield wrong results as this oscillating flow may greatly impact the heat transfer behaviour (Kamsanam, et al., 2015). Due to time and spatial factors, which create cyclic variation of the flow condition, the analysis of oscillatory flow is much more complex compared to steady flow (Jalil, 2019). However, oscillatory flow allows for removal of heat quickly and efficiently.

2.3.1 Convection

The major mode of heat transfer in oscillatory flow is convection heat transfer. Convection is the mode of heat transfer by which the energy transfer is both due to random molecular diffusion (conduction) and also due to the bulk motion of the fluid (Incropera, Dewitt, Bergman, & Lavine, 2007). If there is no bulk motion of the fluid, heat transfer is purely through conduction. The motion of the fluid greatly increases the rate of heat transfer, due to warmer and cooler chunks of fluid are in contact with the surface. In other words, the higher the fluid velocity, the higher the rate of heat transfer. Other flow phenomenon that effect the heat transfer rates are stagnation, separation, reattachment, and vortex formation (Yoo, Kwon, & Kim, 2007).

As mentioned earlier, heat transfer through convection plays an important role in the oscillatory flow. The convection heat transfer coefficient, h , contributes towards convection heat transfer. Eq. (3) shows the convection heat transfer coefficient with a unit heat per unit surface area per unit temperature

$$h = \frac{\dot{Q}}{A(T_{LMTD})} \quad (3)$$

where, h = convection heat transfer coefficient ($\text{W}/\text{m}^2\cdot\text{K}$),

\dot{Q} = rate of heat convection (W),

A = area of heat transfer (m^2),

T_{LMTD} = Log mean temperature difference (K),

where T_{LMTD} is given by,

$$T_{LMTD} = \frac{\Delta T_i - \Delta T_e}{\ln \frac{\Delta T_i}{\Delta T_e}} \quad (4)$$

where, ΔT_i = temperature difference at the inlet (K),

ΔT_e = temperature difference at the outlet (K).

2.3.2 Nusselt Number

In convection studies, the practice to convert the governing equations into a dimensionless parameter is very common. It helps to simplify the calculations and reduces the total number of variables. The variables are grouped together and are called dimensionless number. In heat transfer studies, it is common to equate heat transfer coefficient, h with the Nusselt number, which is viewed as the dimensionless convection heat transfer coefficient and is represented as shown in Eq (5),

$$Nu = \frac{hL_C}{k} \quad (5)$$

where Nu is Nusselt number, h is convection heat transfer coefficient ($\text{W}/\text{m}^2\cdot\text{K}$), L_C is the characteristic length (m), and k is the thermal conductivity of the material ($\text{W}/\text{m}\cdot\text{K}$). The dimensionless parameter was named after Wilhelm Nusselt (1882 – 1957), a German engineer

who made great contributions to convective heat transfer in the first half of the twentieth century (Cengel & Ghajar, 2015). The Nusselt number expresses the ratio of heat transfer through convection in the fluid layer relative to the conduction across the same fluid layer. In other words, the larger the Nusselt number, the larger the heat transfer due to convection. Heat transfer by pure conduction is represented by Nusselt number of $Nu = 1$.

For flow over cylinders and spheres, it commonly involves with flow separation, which is complex to solve analytically. Therefore, these types of flows should be handled experimentally or numerically. The flow patterns across a cylinder can be quiet complex and greatly influences heat transfer. Figure 2.6 illustrates the variation of local Nusselt number Nu_θ around the surface of the cylinder which is subjected to cross flow of air.

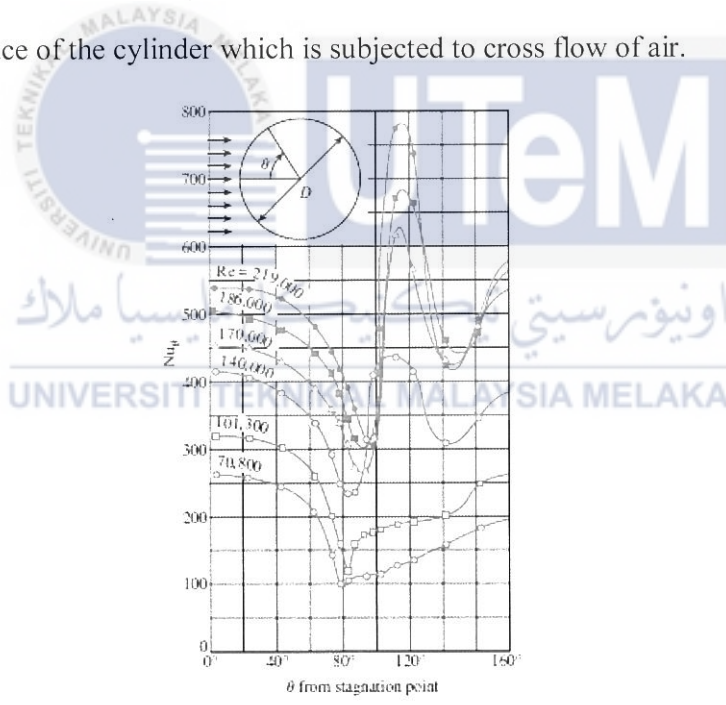


Figure 2.7: Local Nusselt number around cylinder subjected to cross flow of air (Cengel & Cimbala, 2017)

At $Re = 70,800$ and $Re = 101,300$, the Nu_θ reaches a minimum at $\theta = 80^\circ$, which indicates the separation point in laminar flow. Proceeding that, the Nu_θ increases as θ increases due to rapid mixing in the separated flow region (the wake). For the remaining

curves with Re between 140,000 and 219,000, they are different from the first two curves due to having to minimum values for Nu_{θ} . The extreme increase in Nu_{θ} at $\theta = 90^{\circ}$ is due to transition from laminar to turbulent. Nu_{θ} decrease again later in the curve due to increasing formation of boundary layer thickness and reaches the second minimum value as the turbulent flow undergoes flow separation. It later increases gradually as θ increases because of intense mixing in the turbulent wake region.

2.3.3 Prandtl number

Named after famous German physicist, Ludwig Prandtl (1875 – 1953) who made great contribution in aeronautics as well as significant contributions to boundary layer theory, the Prandtl number is a dimensionless parameter that relates the thickness of the velocity and the thermal boundary layer. Eq. (6) describes Prandtl number

$$Pr = \frac{\text{Molecular diffusivity of momentum}}{\text{Molecular diffusivity of heat}} = \frac{\nu}{\alpha} = \frac{\mu C_p}{k} \quad (6)$$

where Prandtl number is Pr , ν is the kinematic viscosity (m^2/s), α is thermal diffusivity (m^2/s), μ is dynamic viscosity ($N \cdot s/m^2$), C_p is specific heat ($J/kg \cdot K$), and k is thermal conductivity ($W/m \cdot K$).

2.3.4 Experimental research on oscillatory flows

The analytical solution for laminar oscillatory flow in pipe was derived by Sexl and later Womersley (Feldmann & Wagner, 2012). The Floquet theory shows that the laminar oscillatory pipe flow and the Hagen–Poiseuille flow is stable for general perturbations but

becomes unstable at higher Womersley number as suggested by Nebauer and Blackburn (2009) and Thomas et al. Hino et al. (1975) used hot-wire anemometry (HWA) analysis to determine the velocity fluid in the pipe. HWA works on the principle of measuring the heat loss of the wire that is placed in the fluid. Placing the wire in the fluid will allow for heat to transfer from the wire to the fluid, which in turn reduces the temperature of the wire. The flow rate of the fluid is indicated by the resistance of the wire.

2.3.5 CFD research on oscillatory flows

Patel and Joshi (2012) conducted a numerical study of the oscillating flow in a circular tube using CFD. They discovered that the velocity profile changes from rectangular shape to parabolic shape due to viscous and inertial effects and there are velocity overshoot occurring near the walls. The “annular effect” becomes great. At high Re_ω , in reciprocating flow, viscous layer does not combine at the fully developed region because of the phase shift of the velocity near the wall and in the core due to inertial effects. Feldmann and Wagner (2016) also contributed in CFD research of oscillatory flow in a pipe by discovering that the tube length is important when simulating oscillatory flow. They discovered that shorter computational domains lead to flow being conditionally turbulent while longer computational domains lead to flow being completely laminarized. Chen et al., (2018) did a numerical study on heat transfer characteristics of oscillating flow in cryogenic regenerators. Their work focuses on the simulation of oscillatory flow and the correlation of heat transfer in screen type generator. The obtained results coincides with steady flow in which heat transfer increases with the increase in Reynolds number. Furthermore, through their simulation, it is observed that the first unit cell shows higher Nusselt number compared to the ones that come after it. The trend

of Nusselt number decreases with the increase in distance of the tubes from the first unit cell. They also concluded that the pulsating flow can increase heat transfer rate even more under high Reynolds number. The increase in oscillating frequency enhances the heat transfer rate which is caused by the small thermal boundary layer thickness in oscillatory flow. Reynolds number has greater impact towards Nusselt number as compared to the effect of oscillation frequency. Oscillatory flow is much more complex than unidirectional flow. Oscillatory flow may undergo the process of relaminarization (Mohd Saat & Jaworski, 2017). Relaminarization is the process where the turbulent-like flow is present, and a laminar-like flow ensues within one cycle.



CHAPTER 3

METHODOLOGY

In this chapter, the framework of the project will be discussed upon in further detail. It covers how the project was implemented and carried out starting from geometry modelling until obtaining the results for further processing and analysis. This chapter also describes the methodology used in this project to achieve data and results for the project.

3.1 Project planning flowchart

This section of the report provides the general idea for the research methodology that is used in this study in order to achieve the objectives of the project. A flowchart is basically visualizing a process using symbols and texts in order to convey the information. Furthermore, the advantages of using a flowchart is that it gives a quick and rough idea of the process flow. It also helps to achieve the targeted objectives in a smooth and orderly manner. In summary, the project was completed using CFD software ANSYS 16.1 and was solved using the commercial CFD package Ansys Fluent 16.1. The model was generated using Ansys Design Modeler. Mesh was generated within the CFD software. Initial condition and boundary condition were applied for oscillatory flow condition and CFD simulation was solved. Figure 3.1 shows the flow of the research methodology with the use of CFD to investigate the oscillatory flow across a tube banks heat exchanger.

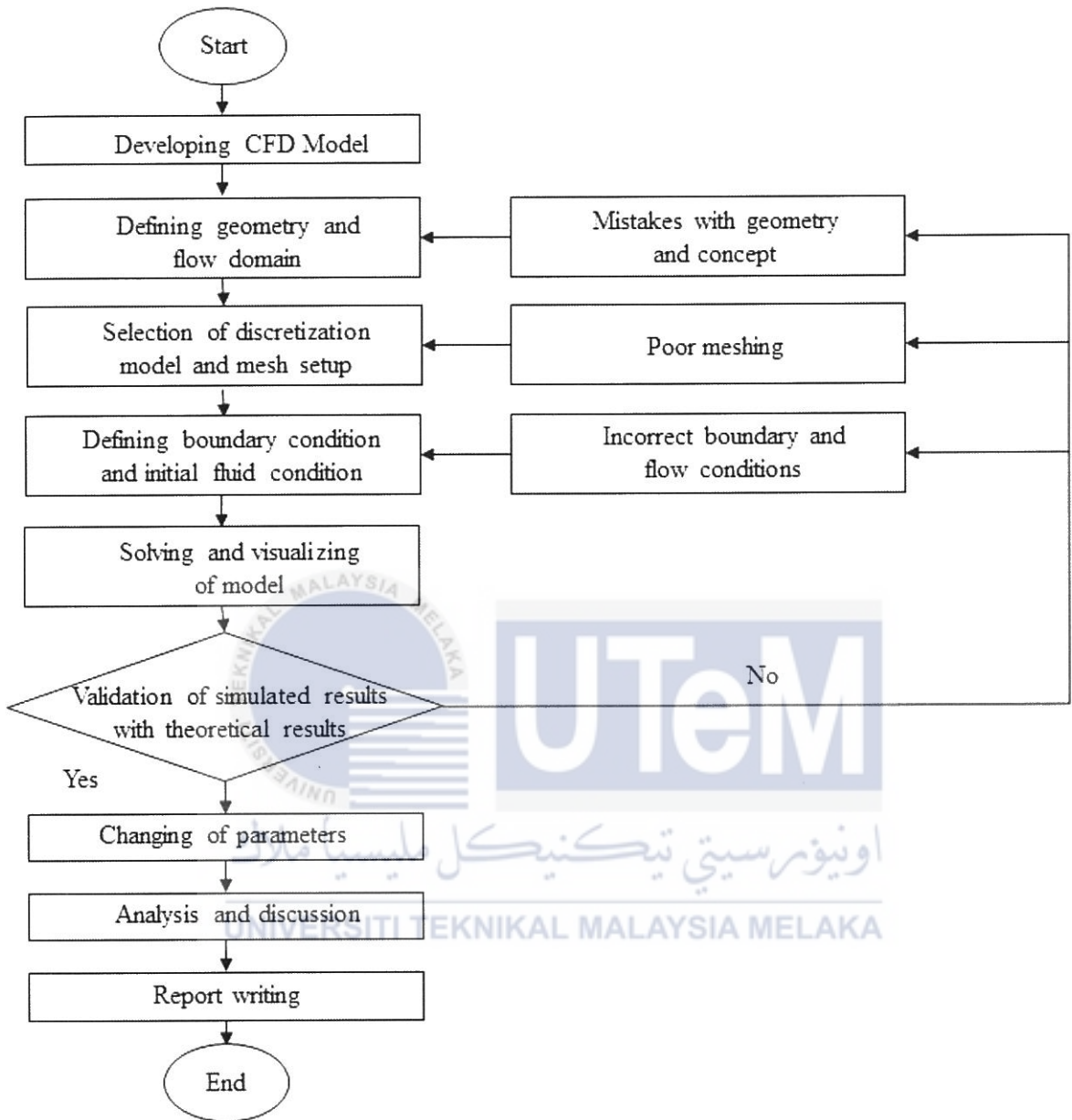


Figure 3.1: Research methodology flowchart

3.2 Developing CFD Model

A two-dimensional (2D) model of a staggered tube bank was produced using ANSYS 16.1. In Ansys Design Modeler, the geometry type was set to 2D analysis type. A sketch of the model was produced using the dimensions listed in Table 3.1.1. The sketch was then converted into a surface layer using the surface from sketches feature. In details of surface body, the details of the geometry were set to fluid type. Figure 3.2 shows the sketch of the 2D staggered tube banks model.

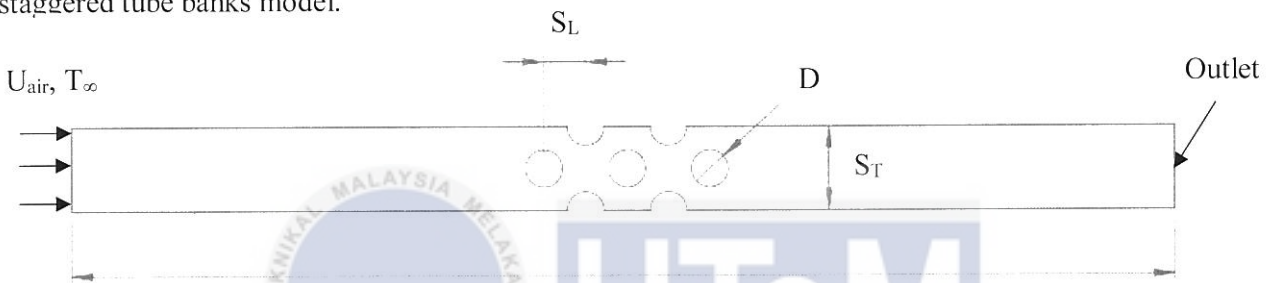


Figure 3.2: Sketch of 2D staggered tube bank model

Table 3.1: Dimensions of the tube banks

Description	Details
Shape of tubes	Circular
Diameter of tube, D (mm)	20
Length of bank array, L (mm)	600
Longitudinal pitch, S_L (mm)	22.5
Transverse pitch, S_T (mm)	45
Angle of attack, θ ($^{\circ}$)	0

3.3 Defining geometry and flow domain

For this numerical simulation, Ansys Fluent 16.1 was used. The first step was to select the Fluent module in the workbench to begin setting up of the flow domain. The geometry model was setup as fluid type computational domain and the named selections were selected as shown in Figure 3.3.

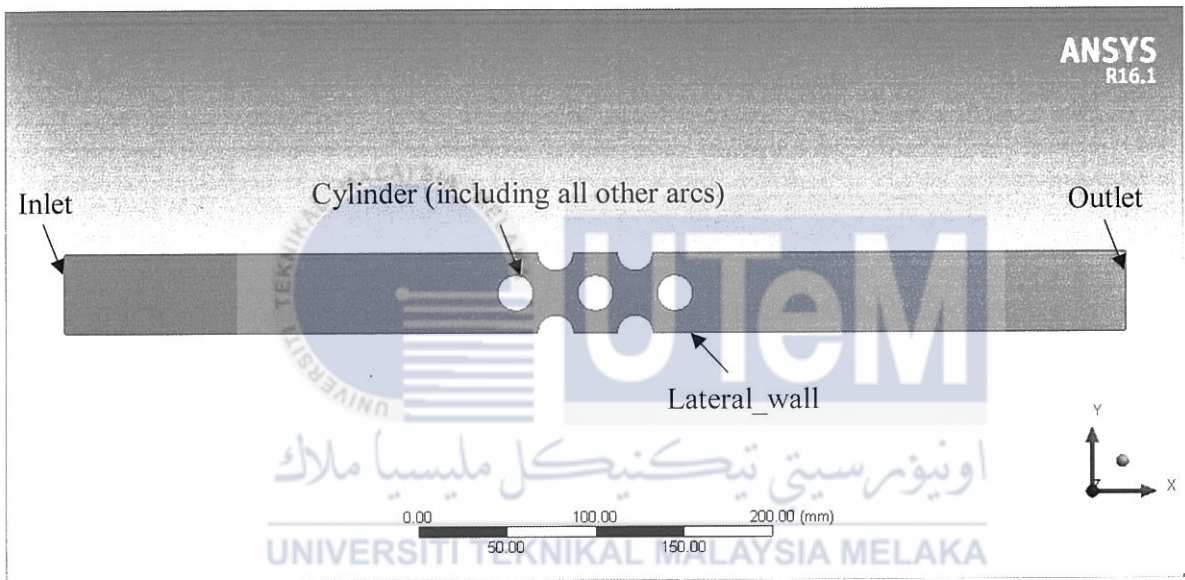


Figure 3.3: Named selections for surface model of tube banks

3.4 Selection of discretization model and mesh setup

Meshing was done using Ansys Meshing. For preliminary meshing, the default sizing method was used on the model to produce the mesh. Table 3.2 shows the details of the mesh sizing option. Figures 3.4 shows the quality of the overall meshing that was produced with the provided settings.

Table 3.2: Details of mesh sizing option

Description	Details
Use advance size function	On: Proximity and Curvature
Relevance center	Fine
Initial size seed	Active assembly
Smoothing	High
Proximity size function sources	Faces and edges
Min size	Default (8.7837e-005 m)
Proximity min size	Default (8.7837e-005 m)
Max face size	Default (8.7837e-003 m)
Max face size	Default (1.7567e-002 m)
Growth rate	Default (1.2)

When generating the mesh, a method was inserted to generate the mesh. The method selected when generating the mesh was the Automatic Method, where the method is Quadrilateral dominant and the free face mesh type is the quad/tri.

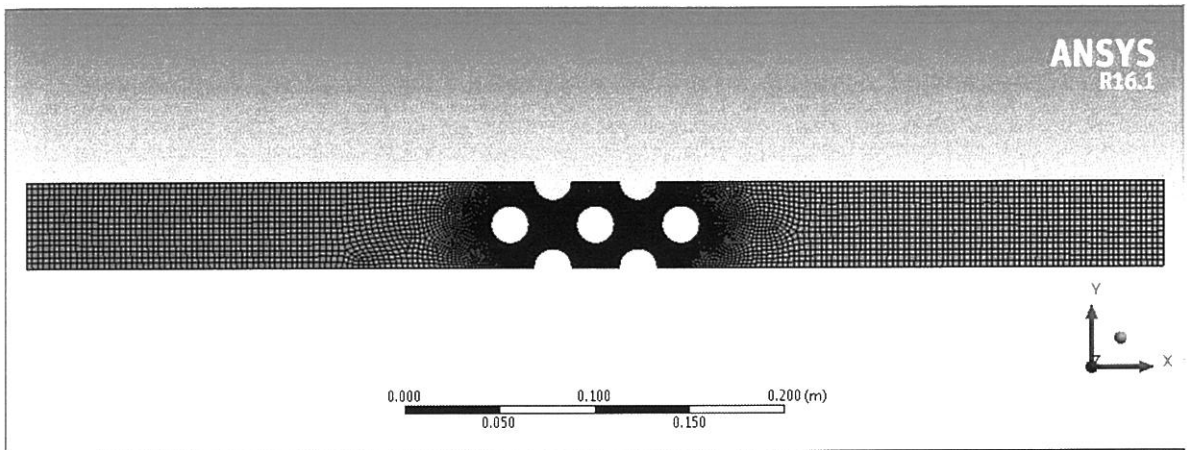


Figure 3.4: Overall meshing

Furthermore, inflation setting was inserted near the walls of the tube cylinder as to obtain a much refined mesh. Inflation option was set to first boundary layer thickness, with a max layers of five layers, and a growth rate of 1.2. Figure 3.5 shows the enlarged picture with inflation near the walls.



Figure 3.5: Enlarged view of mesh around the tube walls (default setting)

Edge sizing was also done to the edges of the tube cylinders. This practice helps in controlling the quality of the mesh within the domain. All seven tube edges were selected and the number of divisions was set to 50 with hard behaviour being set. Figure 3.5 shows the edge sizing.

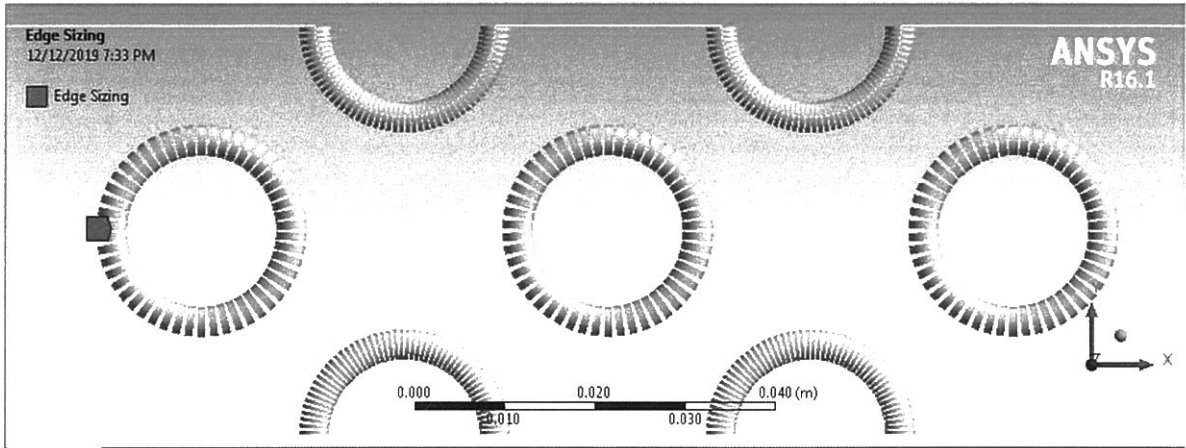
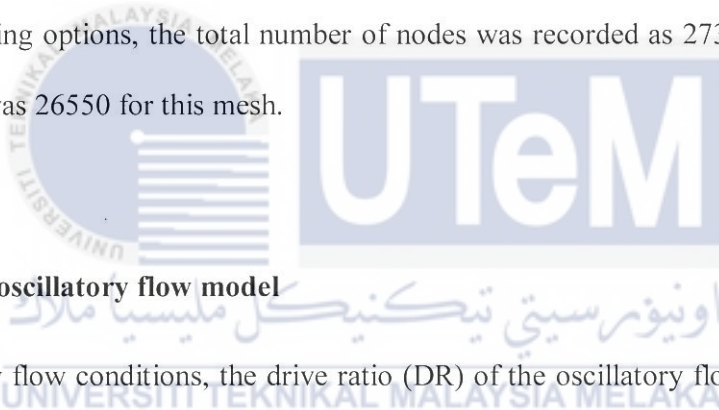


Figure 3.6: Edge Sizing

By using these meshing options, the total number of nodes was recorded as 27370 while the number of elements was 26550 for this mesh.



3.5 Setting up of oscillatory flow model

For oscillatory flow conditions, the drive ratio (DR) of the oscillatory flow was set to 1.2%. Drive ratio is defined as the ratio between the maximum amplitude of pressure to the mean value of pressure. In this model, the DR represents strength and flow amplitude. The frequency of the model was set to 14.2 Hz. Equations (7) and (8) is used to govern the conditions of the inlet and outlet boundaries for the model:

$$P = P_a \cos(kx_1) \cos(2\pi ft) \quad (7)$$

$$m' = \frac{P_a}{c} \sin(kx_2) \cos(2\pi ft + \theta) \quad (8)$$

where P is pressure, P_a is the maximum pressure at the antinode location, k is a wave number given by Equation (10), f is frequency, t is time, m' is mass flux, θ is the phase shift between

pressure and velocity which was set as 1.57 radian for standing wave condition, and c is the speed of sound which is 346m/s.

$$\text{Drive ratio, } DR = \frac{P_a}{P_m} \quad (9)$$

The term P_m is the mean pressure which is also the atmospheric pressure of 100000Pa.

$$\text{Wave number, } k = \frac{2\pi ft}{c} \quad (10)$$

Locations x_1 and x_2 are determined by locating the center of domain to a location of 0.18λ from the pressure antinode location. The term λ is the wavelength and can be determined from Equation (11).

$$\text{Wavelength, } \lambda = \frac{c}{f} \quad (11)$$

The tube banks is located at the centre of the model. This location of 0.18λ is then offset to both ends of the bank array with distances of 300 mm from the center. The values for x_1 and x_2 are 4.086m and 4.686m. The boundary conditions and fluid properties for oscillatory flow is shown in Table 3.3 and Table 3.4 respectively.

Table 3.3: Boundary conditions

Location	Boundary Condition
Inlet	Pressure inlet, DR = 1.2%
Outlet	Mass flux outlet, DR = 1.2%
Tube wall	No slip
Lateral wall	Symmetry

Table 3.4: Fluid properties

Material	Properties	Value
Air	Density, (ρ_{air})	Ideal gas
	Specific heat, ($C_{p_{air}}$)	1006.43 J/kg·K
	Thermal conductivity, (λ_{air})	From Equation (12)
	Viscosity, (μ_{air})	From Equation (13)
	Prandtl number, (Pr)	0.71289
	Inlet temperature, (T_{air})	35 °C
Tube bank walls (Aluminium)	Density, (ρ_t)	2700 kg/m ³
	Heat capacity, (C_{p_t})	879 J/kg·K
	Thermal conductivity, (λ_t)	229 J/kg·K
	Tube temperature, (T_t)	10 °C

Thermal conductivity of air for the oscillatory flow is governed by the piecewise-polynomial method that varies with temperature and is given by Equation (12):

$$\begin{aligned}
 k = & 0.023635 + 7.56264 \times 10^{-5}T - 2.51537 \times 10^{-8}T^2 + 4.18521 \times 10^{-12}T^3 \\
 & + 1.05973 \times 10^{-15}T^4 - 1.21111 \times 10^{-18}T^5 - 5.47329 \times 10^{-22}T^6 \\
 & - 9.94835 \times 10^{-26}T^7
 \end{aligned}
 \tag{12}$$

Viscosity of the air in the oscillatory flow is calculated using the power-law model where temperature is used. Equation (13) shows the viscosity of air:

$$\text{Viscosity, } \mu = 1.85 \times 10^{-5} \left(\frac{T}{T_0}\right)^{0.76}
 \tag{13}$$

where T_0 is the value of the reference temperature of 300K.

3.6 Solving and visualizing of oscillatory model

Solving of the oscillatory flow is done in ANSYS FLUENT. Fluid flow and heat transfer characteristics of flow over the tube walls were solved using continuity, momentum, and energy equations. Double precision was used for the simulation. Pressure based solver was used in the simulation along with transient time. A gravitational acceleration of -9.81m/s^2 was adopted at the Y-axis in consideration of natural convection effect. Energy equations were solved in order to study heat transfer characteristics. The viscous model chosen was the SST k- ω turbulence model with low Re-correction. SST k- ω was used in the solution because it uses both k- ϵ and k- ω models appropriately (Mohd Saat & Jaworski, 2017). This is because SST k- ω model takes into consideration flows that involve both inviscid and viscous region, meaning to say it applies the correct model depending on the distance to the walls. Viscous heating effect was chosen in order to obtain a more accurate turbulent results as well as more accurate thermal properties near the tube walls.

For the pressure-velocity coupling, the algorithm used was the Pressure-Implicit with Splitting Operators (PISO) algorithm as it provides a better solution for transient cases (Mohd Saat & Jaworski, 2017). In the spatial discretization section, the gradient scheme that was chosen was the least square cell based scheme. Pressure, momentum, turbulent kinetic energy, specific dissipation rate, and energy scheme were all solved using second order upwind scheme. First order implicit was used in the transient formulation. In solution initialization, hybrid initialization was used in the initialization method.

The time step size of the solution parameter was determined by $1/(1200f)$ per cycle (Mohd Saat & Jaworski, 2017). This time step size was chosen so that the solution converges within 20 iterations for every time step. The model was solved for a minimum of five

complete cycles in order to achieve high accuracy. Therefore, a time step of 7000 was used and the simulation was solved for a minimum of 70000 iterations.

3.7 Grid test

Grid convergence test or grid independency test is the process of obtaining a more accurate result by computation of successively finer grids. As the mesh becomes finer, the calculation should approach closer to the correct answer. A proper mesh study needs to be conducted in order to obtain the most accurate result. Conducting research on a bad mesh may lead to wastage of computational resources and a skewed solution. The difference in the solutions obtained from the different refinements are considered to be the accuracy of the coarser grid (Svärd, 2014). If there are no significant changes to the solution after further mesh refinement (or other changes), then the mesh is considered to be grid independent as the grid does not have significant impact on the solution. There are several ways to increase the refinement of the mesh. The ones that are used in refining the mesh in this study are refining the surface mesh, and inflation of the meshing at the edge. In this study, three different mesh sizes were tested for grid independency study.

3.7.1 Mesh quality

The determining factors that contribute to the quality of the mesh are the aspect ratio, the orthogonal quality, and the orthogonal skewness.

Table 3.5: Mesh quality of grids

Study no.	Number of elements	Aspect ratio	Minimum orthogonal quality (close to 0 corresponds to low quality)	Orthogonal skewness (close to 1 corresponds to low quality)
1	26550	2.3359	0.63612	0.62988
2	51253	7.9084	0.68407	0.57451
3	98693	7.8331	0.57711	0.65444

3.7.2 Grid independency test

The mesh test was carried out using the meshes that were defined in Section 3.7.1. The drive ratio chosen for this mesh test was at drive ratio 1.2% for oscillatory flow model. Figures 3.7 and 3.8 show the change for velocity and pressure against time for the tested grid sizes for the duration of one acoustic cycle. The determining factors that contribute to the quality of the mesh are aspect ratio, orthogonal quality, and orthogonal skewness.

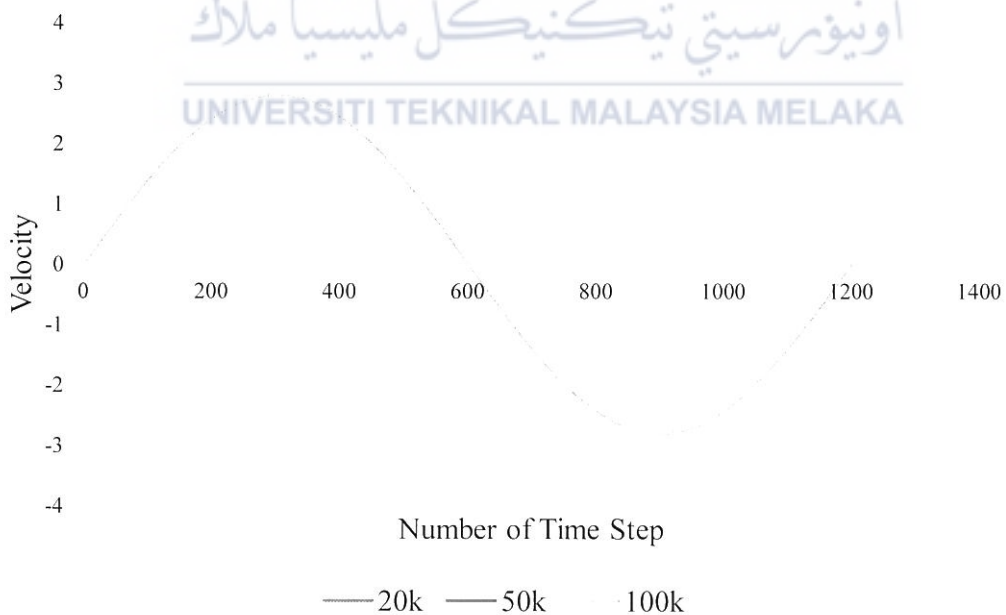


Figure 3.7: Graph for oscillating velocity at DR 1.2%

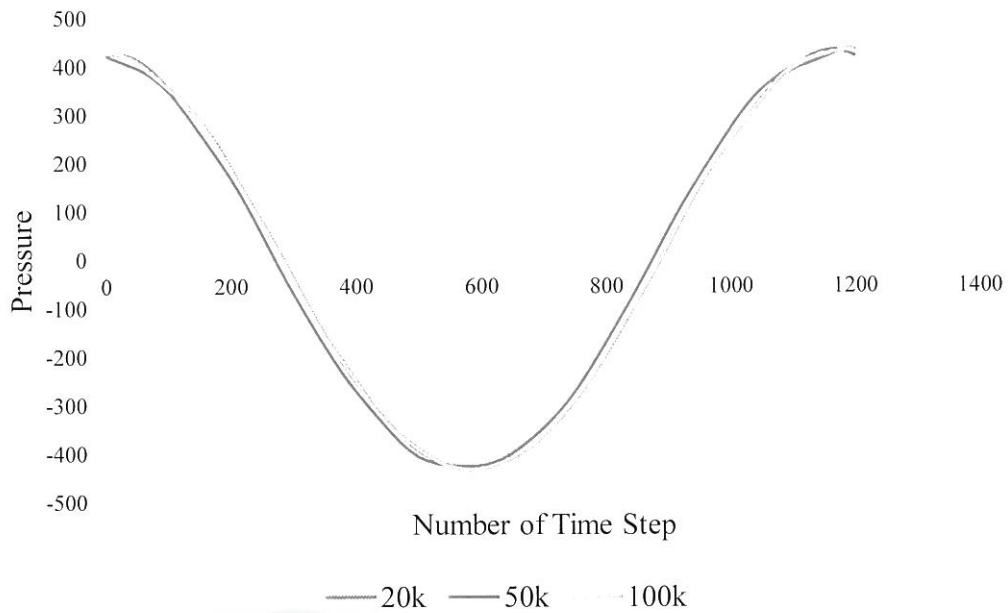


Figure 3.8: Graph for oscillating pressure at DR 1.2%

By comparing both graphs for the velocity and pressure oscillations at three different mesh elements, it is observed that there are no large fluctuations between the different sizes of meshes. The results are independent of the mesh sizes if the number of elements are higher than 20000.

3.7.3 Grid selection

For selection of the proper grid for the simulation, the aspect ratio, minimum orthogonal quality, and maximum orthogonal skewness were examined. Aspect ratio is defined by the measure of how much the cells are stretched. In flows where the bulk of the fluid is moving (near the walls), it is advised to keep the aspect ratio of below 5:1. However, in most cases, an aspect ratio of 10:1 can be used for cells that are near the boundary layer.

The aspect ratio can go as high as possible with regards to the stability of the flow solution. However, when considering the stability of the energy solution, ideally the aspect ratio should not be greater than a ratio of 35:1 (ANSYS FLUENT 12.0/12.1 Documentation, 2009). Another value in which it is used to determine the proper selection of grid is the orthogonal quality. The range for orthogonal quality is from 0-1, where a value of 0 is worst and a value of 1 is the best. Therefore, the closer the orthogonal quality is it to the value of 1, the more accurate results can be achieved. The last measure of determining a good mesh quality is the orthogonal skewness. Skewness of a cell is determined by taking the difference between the shape of the cell and the shape of an equilateral cell of the same volume (ANSYS FLUENT 12.0/12.1 Documentation, 2009). Table 3.6 shows the range of value of skewness and the respective cell quality.

Table 3.6: Range of skewness and cell quality (ANSYS, Inc., 2020)

Value of Skewness	Cell Quality
1	degenerate
0.9 — <1	bad (sliver)
0.75 — 0.9	poor
0.5 — 0.75	fair
0.25 — 0.5	good
>0 — 0.25	excellent
0	equilateral

From the definition of skewness, a value of closer to 0 indicates a low skewness value which would yield a more accurate result, while a value of 1 indicates a completely degenerate cell (worst).

CHAPTER 4

RESULTS AND DISCUSSIONS

Validation of results is important in any investigations. It determines whether the results obtained are correct, valid, and useful for future uses and references. There are various ways for validation to be done. Examples are reviewing previous works, publications, journals, or correlation with theoretical values.

4.1 Validation of oscillatory flows

For validation of the oscillatory flows, a comparison was made between the CFD results obtained against the theoretical prediction of linear thermoacoustic theory. For each drive ratio, DR, the point at which data was collected is at 0.2 m from the center of the model. Using Equation (10) discussed in the previous chapter, distance of the data collection point, x_p , from the pressure antinode, P_a , was calculated to be $x_p = 4.5866\text{m}$. Figure 4.1 shows a graph of comparison of results between theory and CFD for oscillating velocity at DR 0.83%.

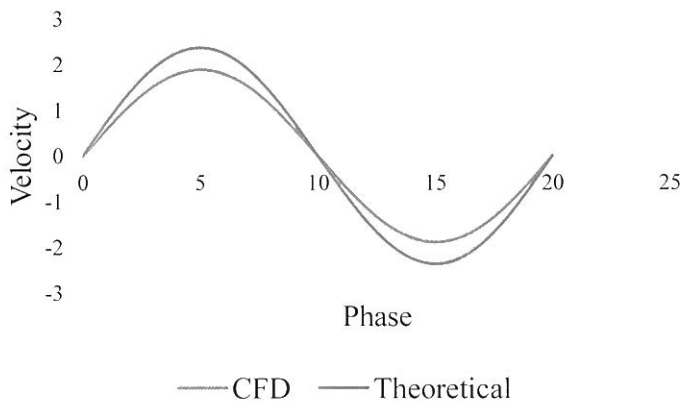


Figure 4.1: Validation of model using velocity oscillation at DR 0.83%

Figure 4.2 shows a graph that shows comparison of results between theory and CFD for oscillating velocity at DR of 1.2%.

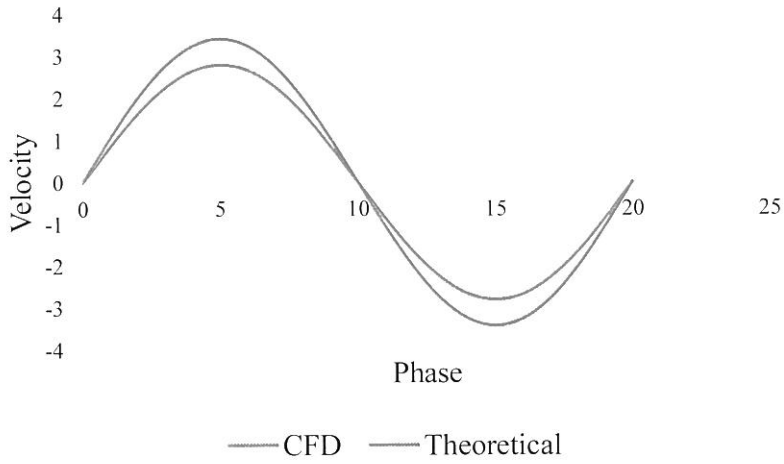


Figure 4.2: Graph comparison of oscillation velocity at DR 1.2%

Figure 4.3 shows a graph of comparison of results between theory and CFD for oscillating velocity at DR 1.5%.

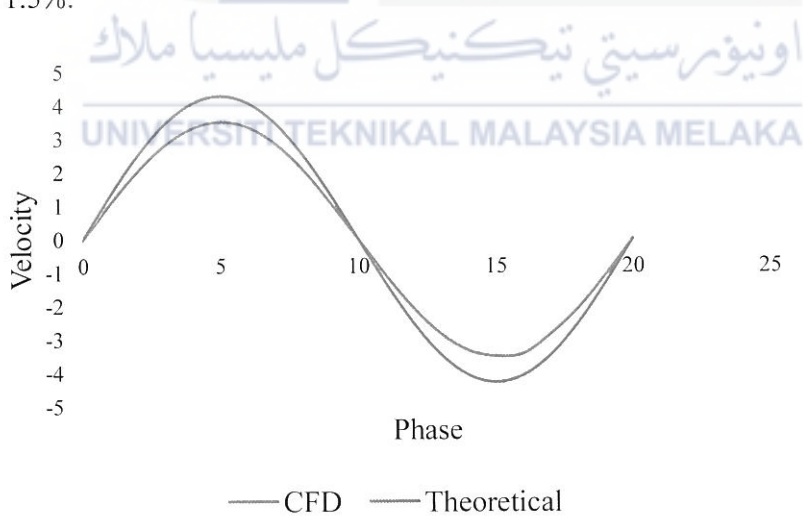


Figure 4.3: Graph comparison of oscillation velocity at DR 1.5%

Figure 4.4 shows a graph of comparison of results between theory and CFD for oscillating velocity at DR 2.0%.

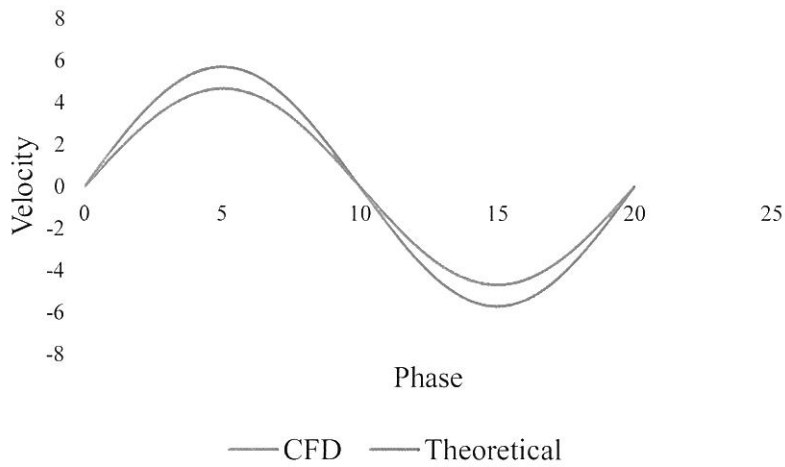


Figure 4.4: Graph comparison of oscillation velocity at DR 2.0%

Based on the observation of results from Figure 4.1 to Figure 4.4, the simulation was modelled fairly accurately and is stable as it did not deviate from the calculated theoretical data. This signifies that the results are valid and further analysis can be done on the model.

4.2 Velocity contour

For this project, the analysis of oscillatory flow conditions was made based on the cyclic behaviour of the flow. Several instantaneous points over a one cycle flow were chosen and data were collected from these points. Figures 4.5 to 4.8 shows the instantaneous points labelled as $\Phi 1$ to $\Phi 20$ for one flow cycle with drive ratios ranging from 0.83% to 2.0%.

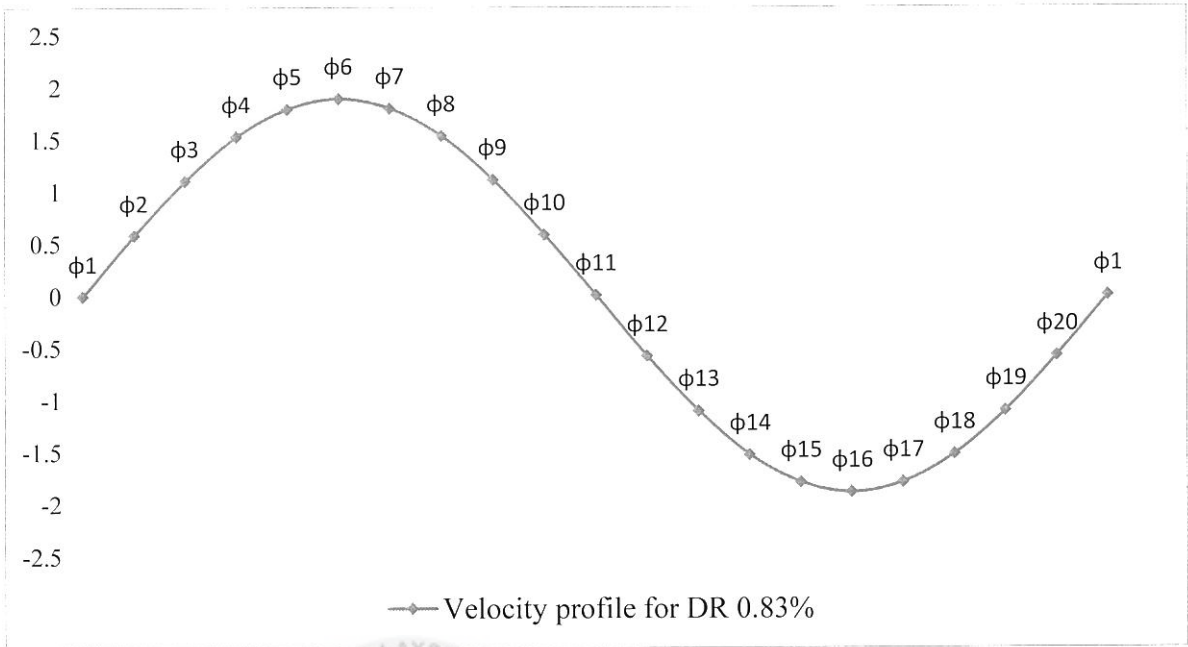


Figure 4.5: Velocity profile for DR 0.83%

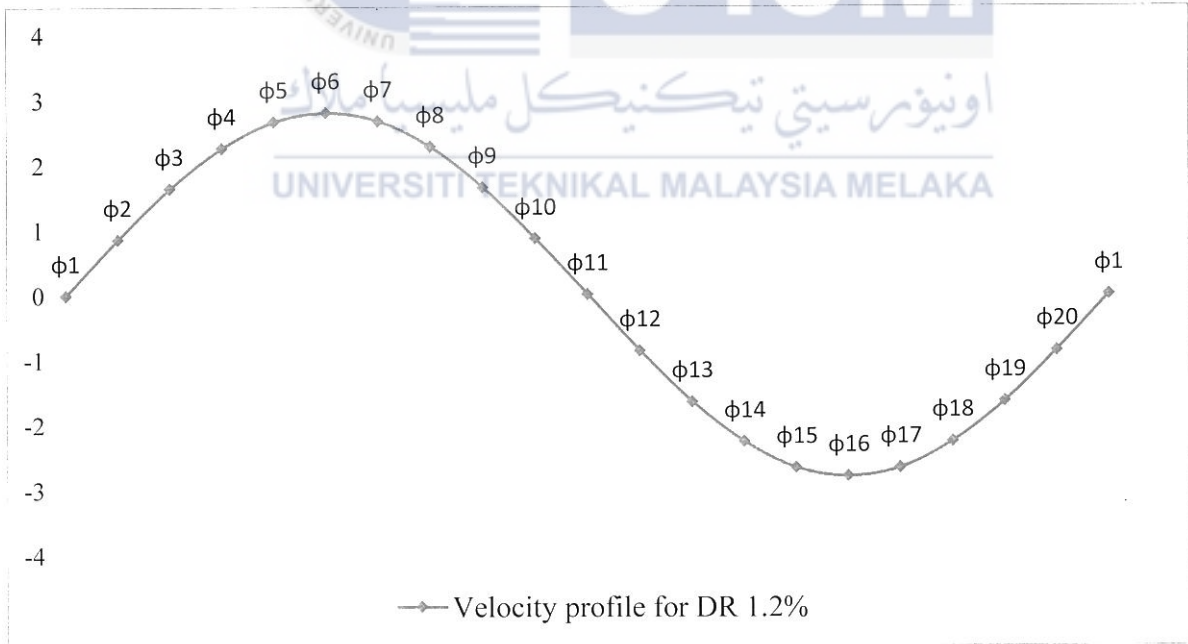


Figure 4.6: Velocity profile for DR 1.2%

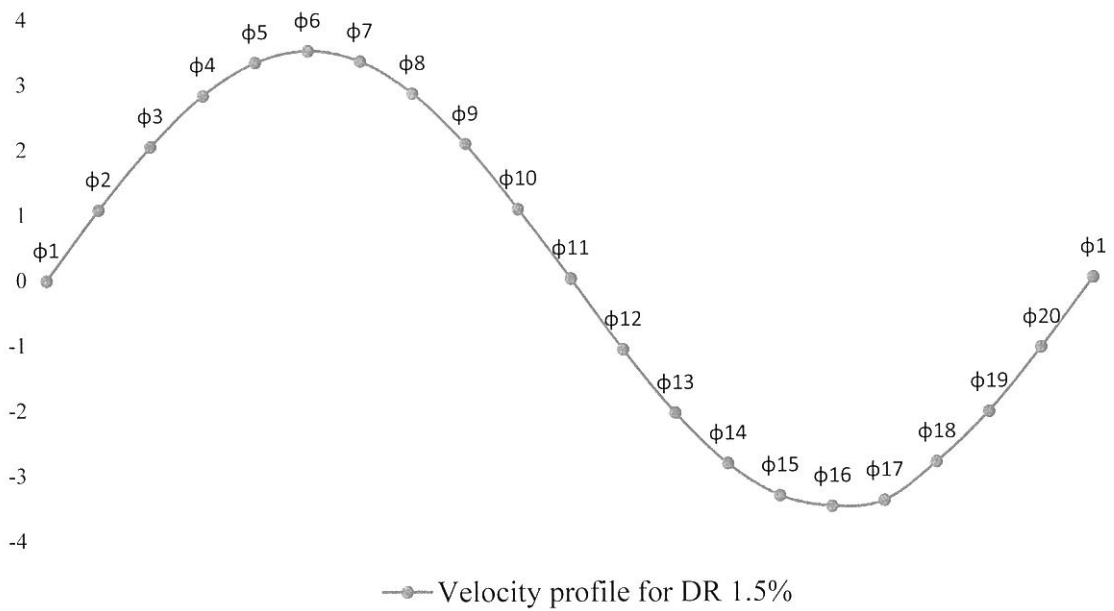


Figure 4.7: Velocity profile for DR 1.5%

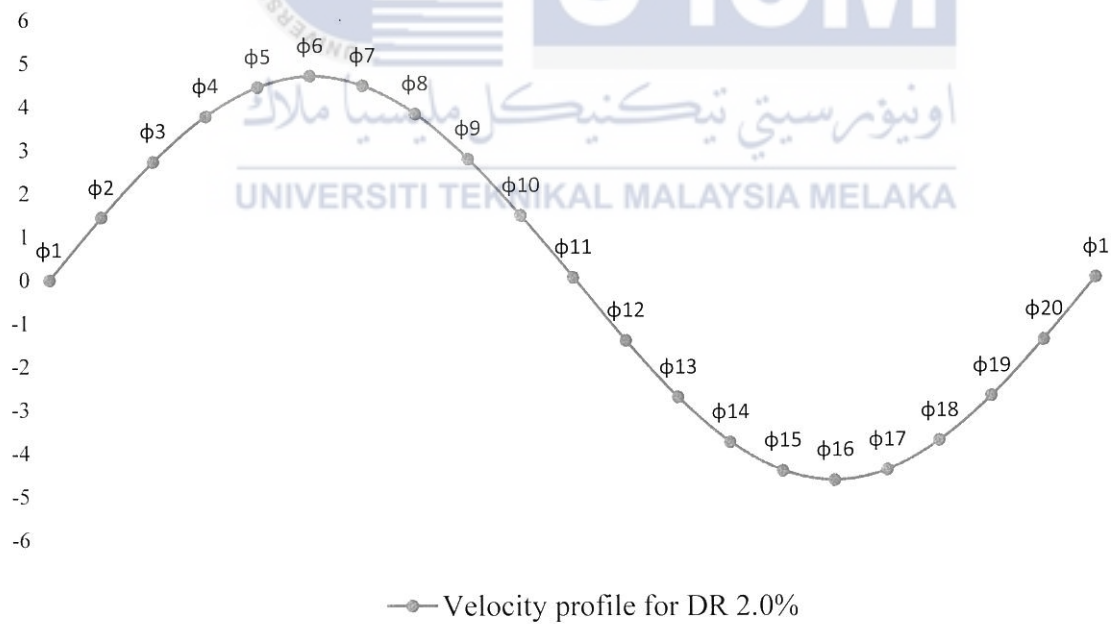
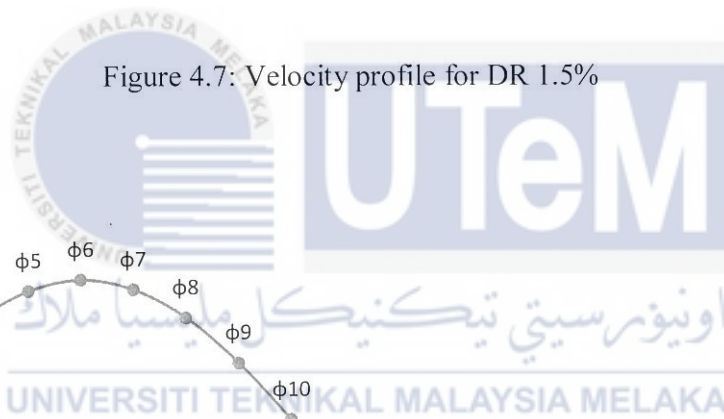


Figure 4.8: Velocity profile for DR 2.0%

From the Figures 4.5 to 4.8, we can generalise that the instantaneous points from $\Phi 1$ - $\Phi 10$ represents the flow moving forward while from $\Phi 11$ - $\Phi 20$ represents the reverse flow. The vector plots are as shown in Tables 4.1 for DR 0.83% and 1.2% and Table 4.2 for DR 1.5% and 2.0%. From results that were obtained, it was noted that the maximum velocity for DR 0.83%, 1.2%, 1.5%, and 2.0% are 6.23 m/s, 9.96 m/s, 10.88 m/s, and 14.48 m/s, respectively.

Table 4.1: Velocity contour for drive ratio 0.83% and 1.2%

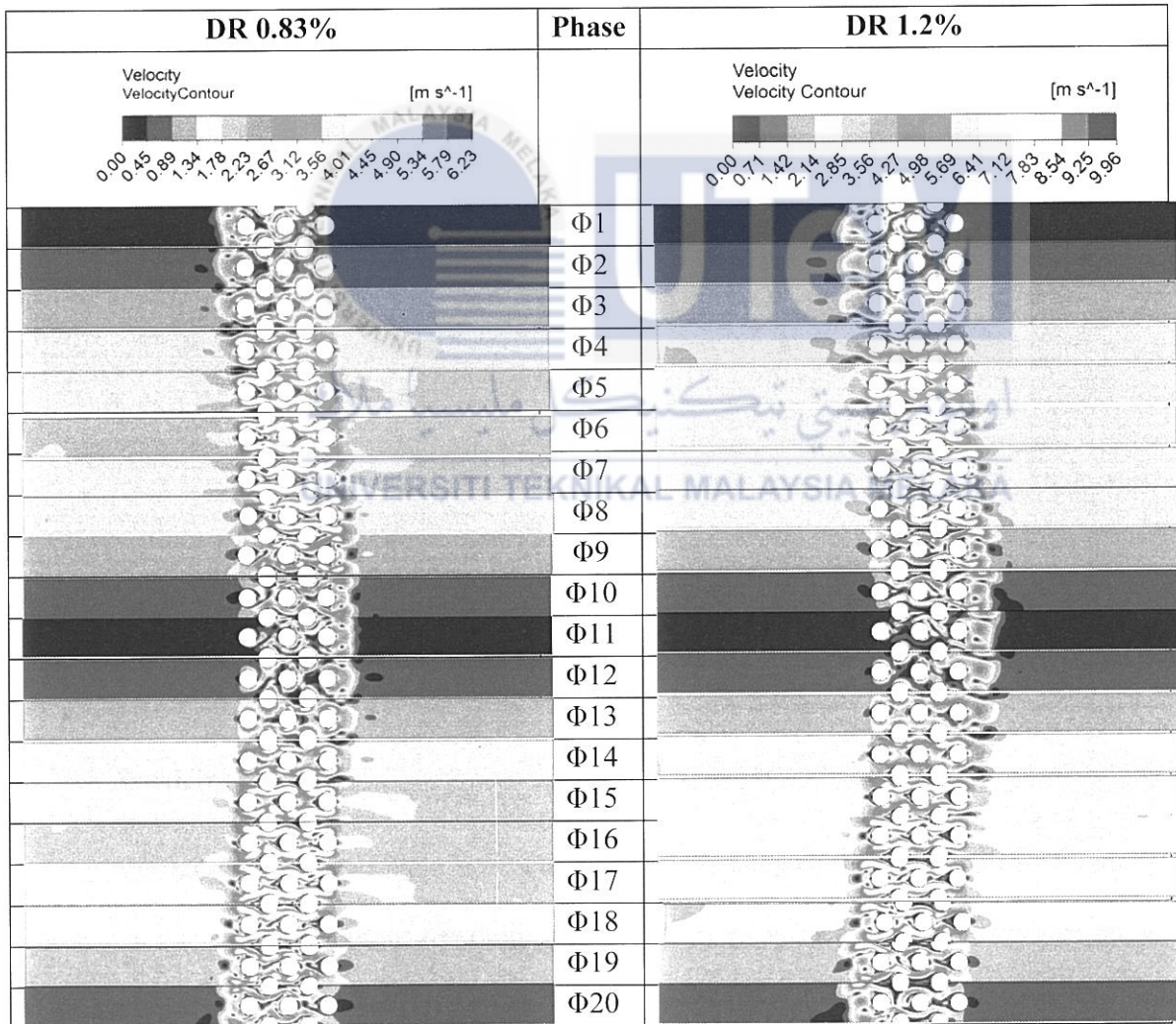
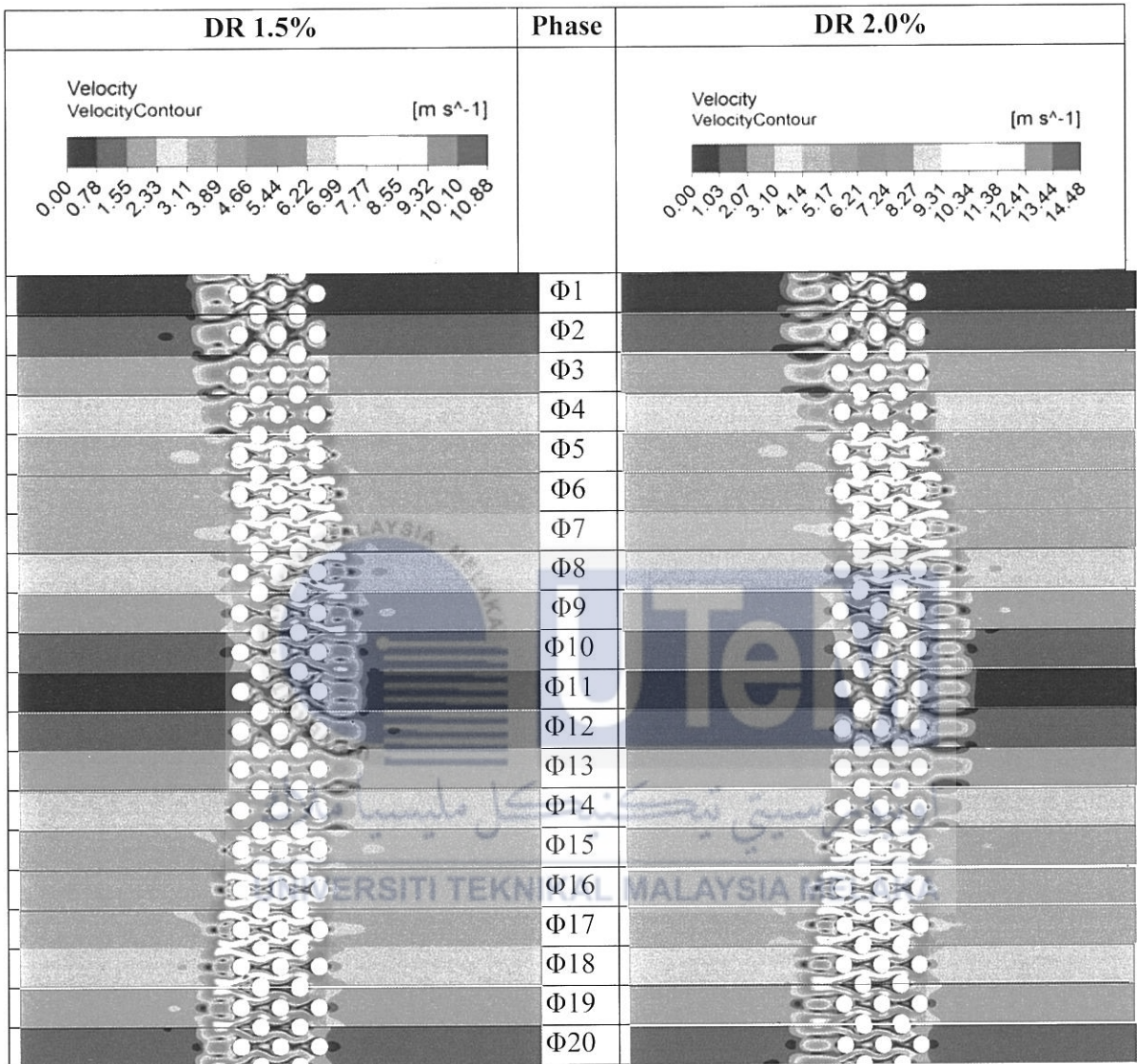


Table 4.2: Velocity contour for drive ratio 1.5% and 2.0%



4.3 Vorticity contour

Vorticity on the other hand is a measure of rotationality of the fluid. In other words, it shows the quality of rotation of the fluid. Tables 4.3 shows vorticity contour for drive ratios 0.83% and 1.2% while Table 4.4 shows the vorticity for drive ratios of 1.5% and 2.0%.

Table 4.3: Vorticity contour for drive ratio 0.83% and 1.2%

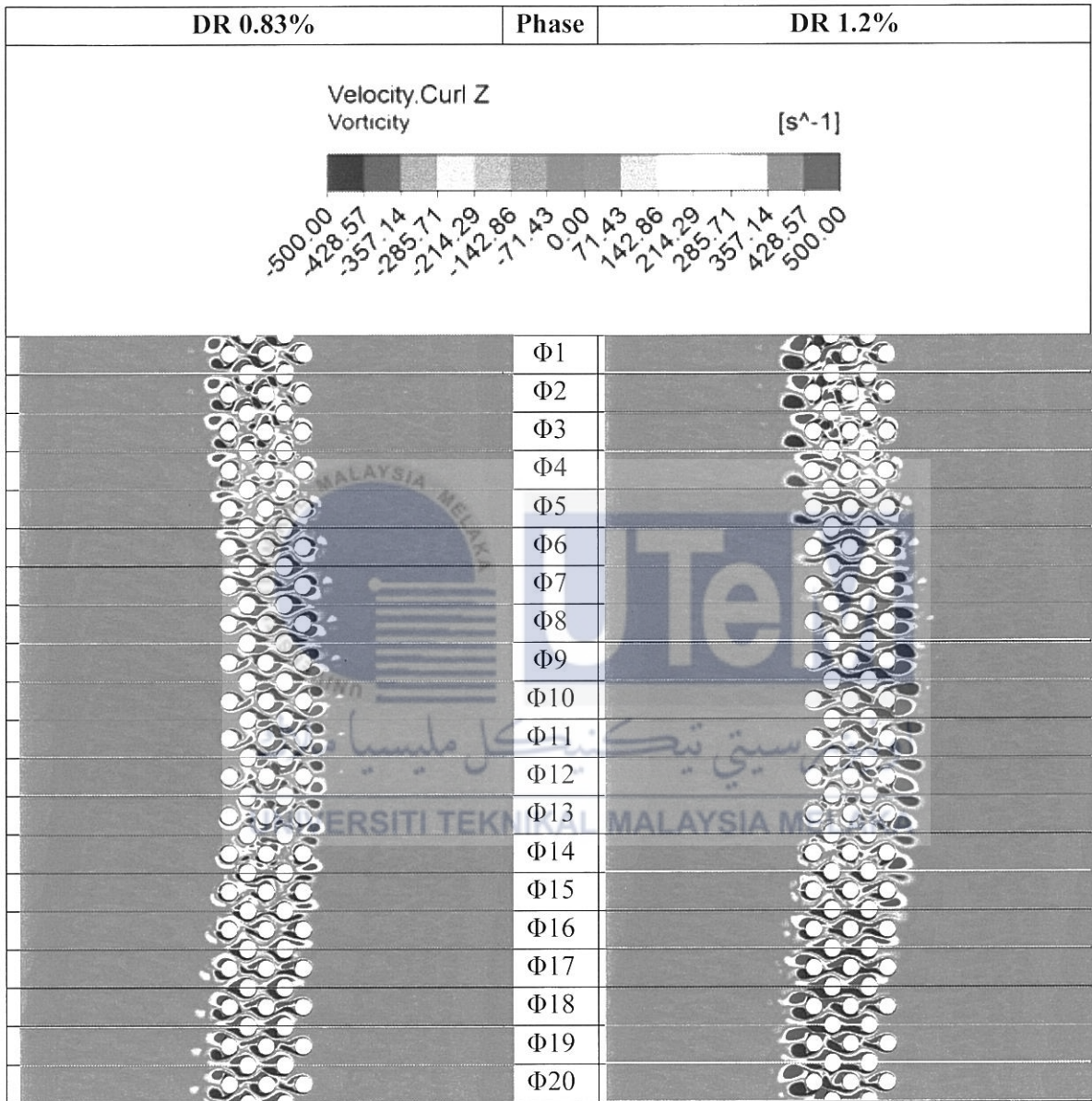
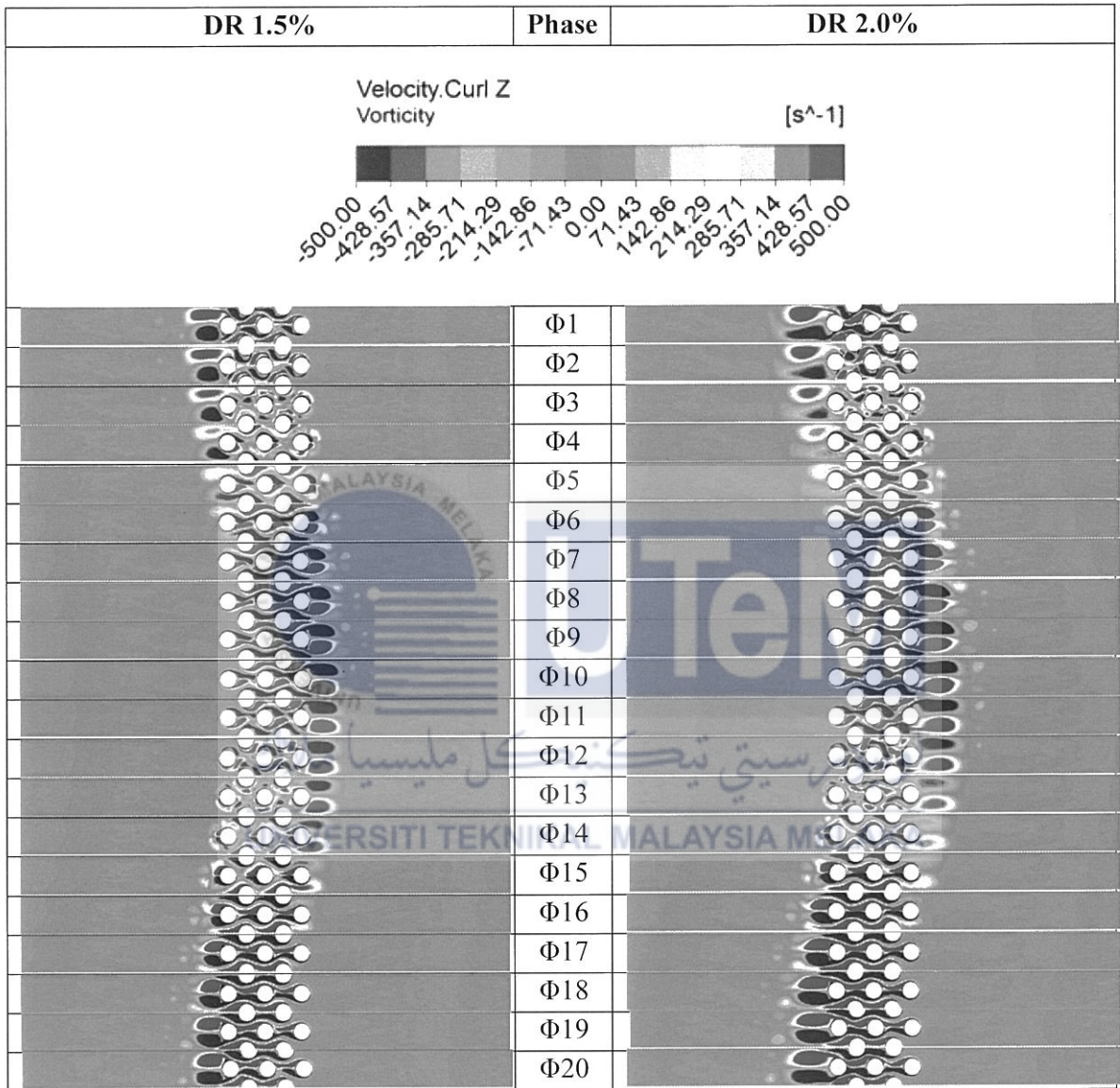


Table 4.4: Vorticity contour for drive ratio 1.5% and 2.0%



When making a comparison between all 4 drive ratios, it is apparent that the higher the drive ratio, there are longer and larger vortices that are formed due to the turbulence behind the tubes as the flow passes by. This is made apparent in all cases especially at Φ1 and Φ11 where the flow is at peak and is about to change direction.

4.4 Temperature contour

Table 4.5 shows the changes of temperature contour of the fluid in oscillatory flow for drive ratios 0.83% and 1.2% and Table 4.6 shows the changes of temperature contour of the fluid in oscillatory flow for drive ratios 1.5% and 2.0%.

Table 4.5: Temperature contour for drive ratio 0.83% and 1.2%

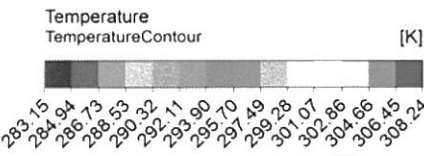
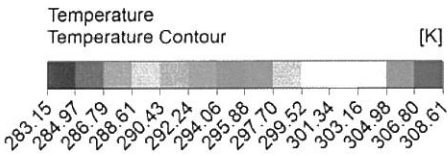
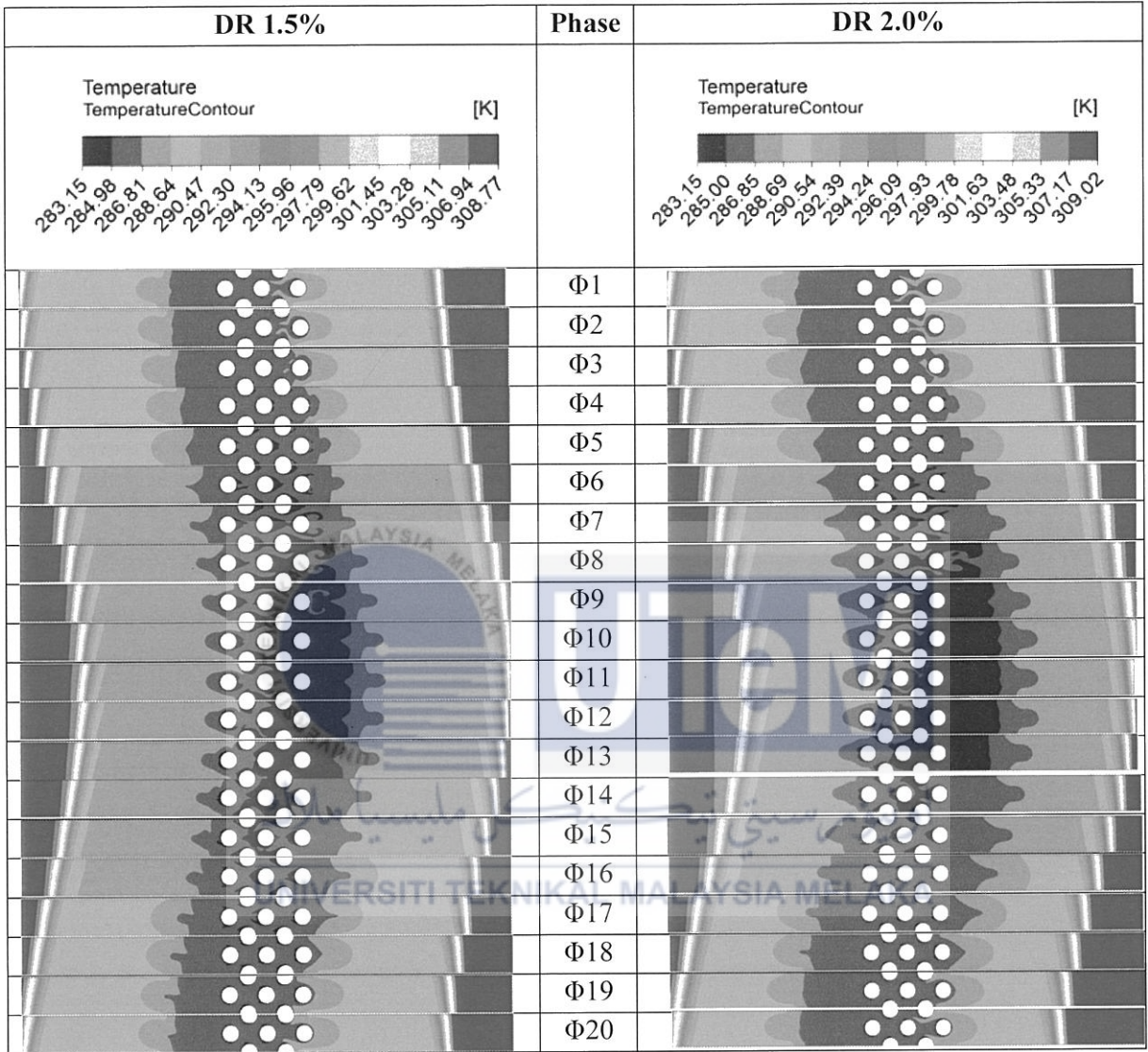
DR 0.83%	Phase	DR 1.2%
 <p>Temperature Contour [K]</p> <p>283.15, 284.94, 286.73, 288.53, 290.32, 292.11, 293.90, 295.70, 297.49, 299.28, 301.07, 302.86, 304.66, 306.45, 308.24</p>		 <p>Temperature Contour [K]</p> <p>283.15, 284.97, 286.79, 288.61, 290.43, 292.24, 294.06, 295.88, 297.70, 299.52, 301.34, 303.16, 304.98, 306.80, 308.61</p>
	Φ1	
	Φ2	
	Φ3	
	Φ4	
	Φ5	
	Φ6	
	Φ7	
	Φ8	
	Φ9	
	Φ10	
	Φ11	
	Φ12	
	Φ13	
	Φ14	
	Φ15	
	Φ16	
	Φ17	
	Φ18	
	Φ19	
	Φ20	

Table 4.6: Temperature contour for drive ratio 1.5% and 2.0%



When comparing the data from all the drive ratio, clearly it is observed that at higher drive ratio, more heat is transferred from external domain of the fluid to the cold tube banks. Maximum heat transfer rate can be seen at Φ11 where the flow is at max peak and is about the change flow direction.

4.5 Pressure contour

Table 4.7 shows the changes of pressure contour of the fluid in oscillatory flow for drive ratios 0.83% and 1.2% and Table 4.8 shows the changes of pressure contour of the fluid in oscillatory flow for drive ratios 1.5% and 2.0%.

Table 4.7: Pressure contour for drive ratio 0.83% and 1.2%

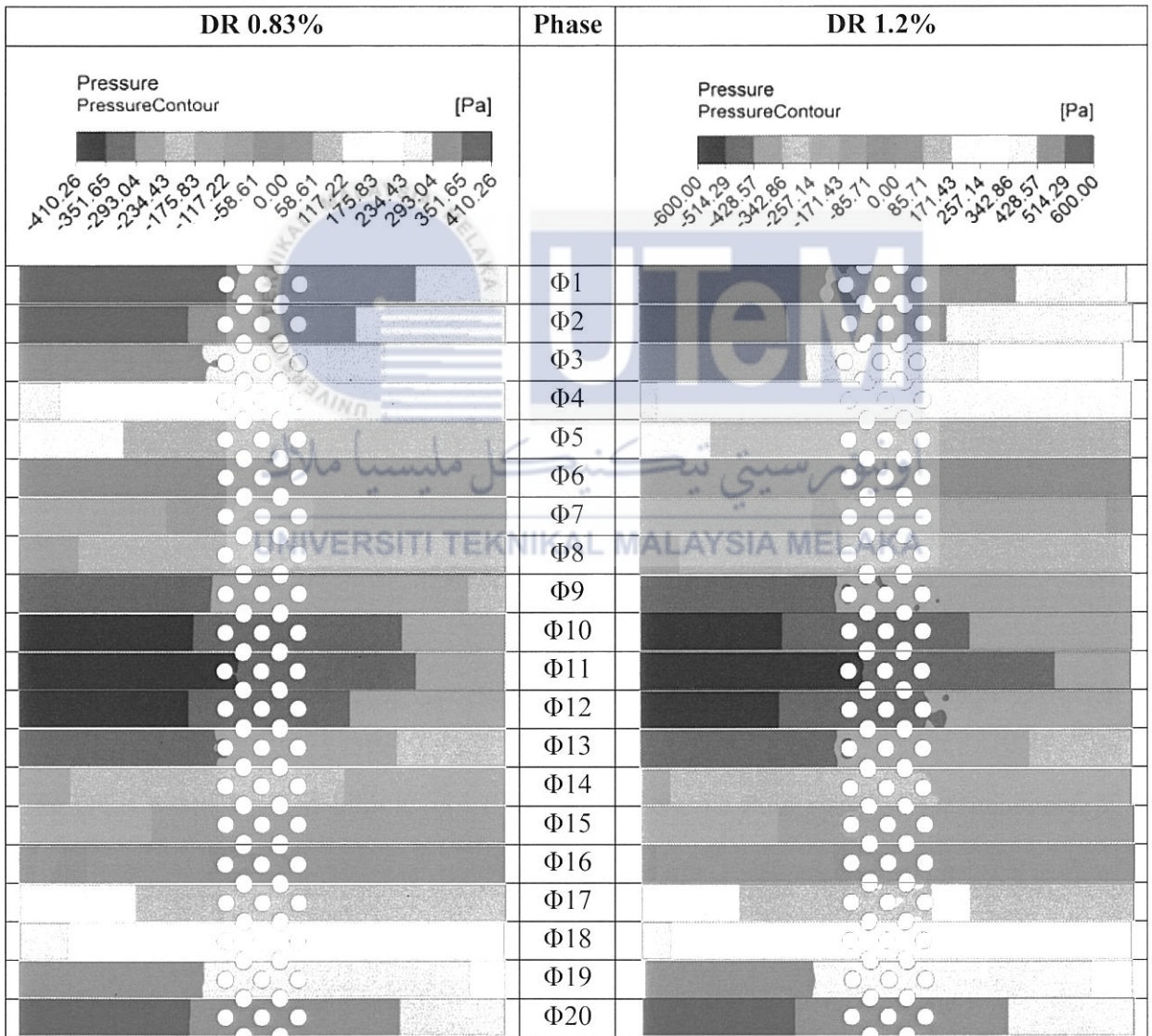
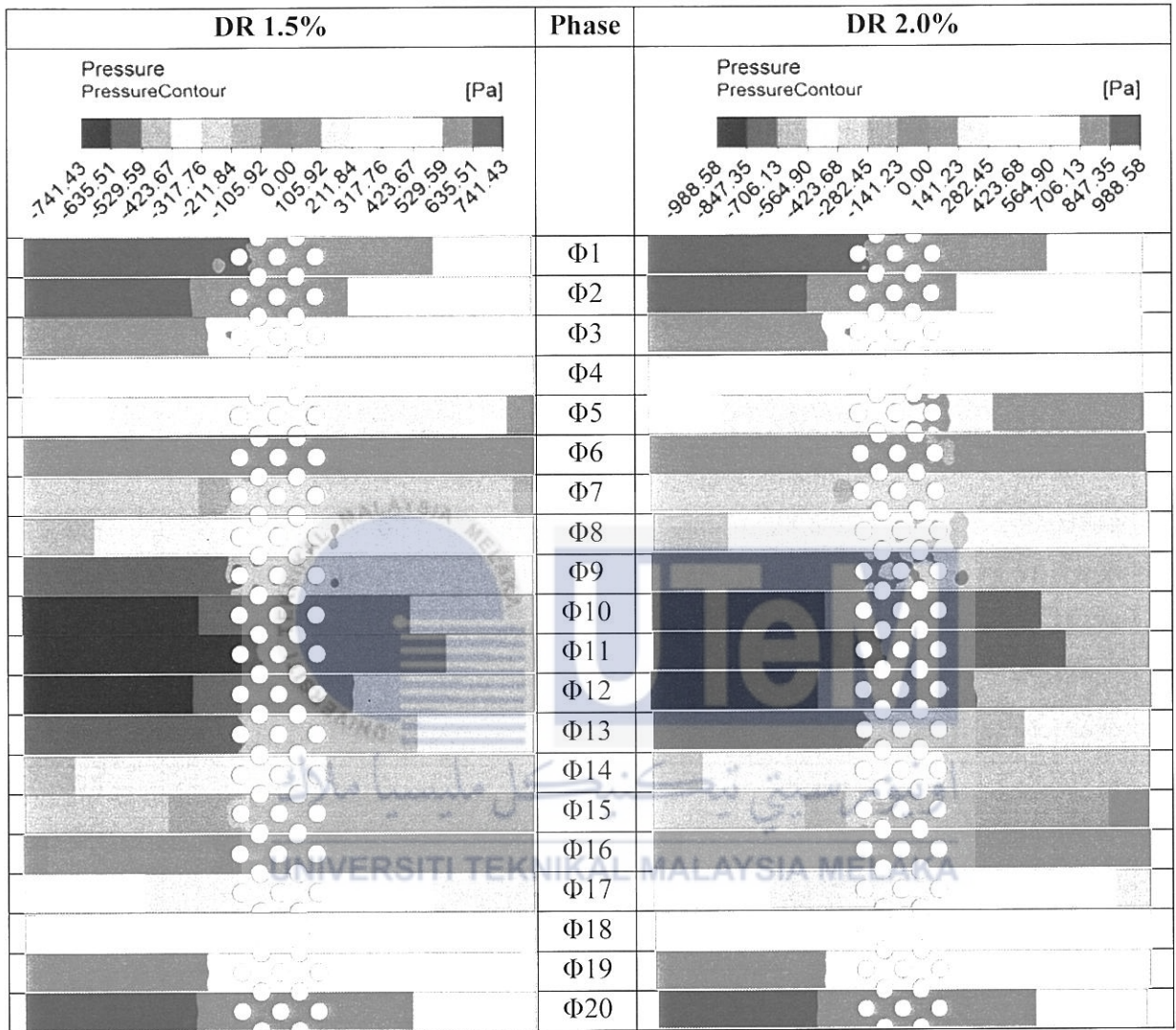


Table 4.8: Pressure contour for drive ratio 1.5% and 2.0%



The pressure amplitude is highest at $\Phi 1$ and $\Phi 20$ where the fluid velocity is at minimum, while lowest at $\Phi 11$ where the fluid velocity is at maximum. These results are consistent with Bernoulli's principle. Even though the contour plot for all drive ratios are similar, the disparity between the minimum and maximum pressure values by the drive ratios suggest that the pressure distribution is affected by the oscillating flow model.

4.6 Heat transfer coefficient

Table 4.9 shows the measure of surface heat transfer coefficient of the cylinder tubes obtained from the flow simulation for oscillatory flow of different drive ratios over 20 phases. The values were obtained using the built-in function of Ansys Fluent 16.1 (Solutions - Reports – Surface integrals – Surface Heat Transfer Coefficient).

Table 4.9: Surface heat transfer coefficient

Phase	Drive Ratio			
	0.83%	1.2%	1.5%	2.0%
Φ1	20.35735	38.264547	41.27915	51.07535
Φ2	19.15723	35.123302	37.88055	46.86702
Φ3	18.56906	34.349141	38.65274	49.03645
Φ4	18.1682	34.863492	40.58372	51.76208
Φ5	17.08113	34.923759	41.61058	52.33338
Φ6	16.94283	34.505032	39.66802	49.38652
Φ7	15.93255	33.821496	37.30997	45.16696
Φ8	15.04404	31.380037	34.40428	39.93954
Φ9	13.92107	29.780708	31.1994	35.44355
Φ10	12.86836	26.134713	27.50105	31.42892
Φ11	12.54751	22.872949	24.65933	27.87564
Φ12	12.3735	22.33418	23.74628	27.34611
Φ13	13.19363	23.996927	26.66501	31.56697
Φ14	14.43303	28.247706	31.99211	38.90748
Φ15	15.96351	32.335979	37.14343	45.71665
Φ16	18.0612	36.220864	40.84491	51.66165
Φ17	19.35588	38.170223	43.92573	54.95688
Φ18	20.36566	40.062222	45.05815	56.19575
Φ19	20.29835	38.968509	44.12971	55.29804
Φ20	19.50054	36.329306	41.07185	51.7485
Average	16.77809	32.62343938	36.47811	44.75861

Heat transfer rate for oscillatory flow over tube banks has no known documented record, and therefore, peak value of inlet temperature was taken and minimum value of outlet temperature was taken for all phases of oscillatory flow models. By using Eq. (3) and Eq. (4), heat transfer rate for all oscillatory flows at all DR can be calculated. Table 4.10 shows the calculated heat transfer rate for all DR while Figure 4.9 shows the heat transfer rate in graphical form. The increase in heat transfer rate depicted from the graph shows that higher DR values yield greater heat transfer as suggested from the temperature contour plots shown in Section 4.4.

Table 4.10: Calculated heat transfer rate

Drive ratio (DR)	0.83	1.2	1.5	2.0
Heat transfer rate, q (W/m ² .K)	0.080527652	0.177237784	0.203403559	0.258498002

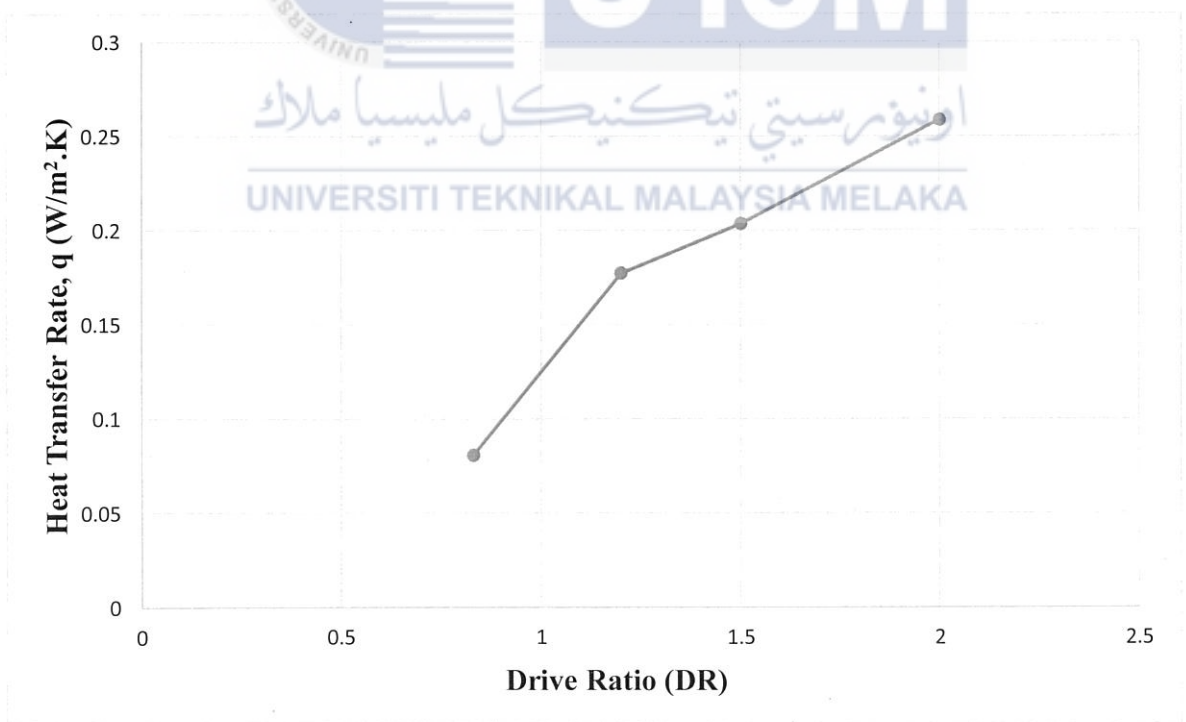


Figure 4.9: Graphical representation of heat transfer rate for different drive ratios.

CHAPTER 5

CONCLUSION AND RECOMMENDATIONS

In conclusion, the objectives of this project were achieved. The CFD model was successfully developed using Ansys Fluent. Mesh independency test was carried out with different grid sizes to obtain accurate results. Results that were obtained from the simulations were then validated using theoretical formulas for oscillatory flows. The fluid flow characteristics for different drive ratios of oscillatory flows were analysed. Contour plots for velocity, vorticity, and pressure were examined for different drive ratios. Heat transfer characteristics were also visualized in the form of temperature contour plots for different drive ratios. The heat transfer coefficient was determined by using the build-in function of Ansys Fluent. It is found that higher drive ratios lead to better heat transfer performance.

In this study, only 2D modelling is focused on where a 3D model simulation may result in higher accuracy of heat transfer and also flow modelling for oscillatory flow. Furthermore, since the oscillatory flow field has yet to be well established, it is suggested that a proper heat equation model should be used when carrying out oscillatory flow models.

References

- ANSYS FLUENT 12.0/12.1 Documentation. (2009, January 29). *6.2.2 Mesh Quality*. Retrieved from ANSYS FLUENT 12.0/12.1 Documentation: <https://www.afs.enea.it/project/neptunius/docs/fluent/html/ug/node167.htm>
- ANSYS, Inc. (2020, May 5). *ANSYS Meshing User's Guide*. Retrieved from Academia: https://www.academia.edu/27974461/ANSYS_Meshing_Users_Guide
- Beale, S. B. (2011, March 16). *THERMOPEDIA™*. Retrieved September 25, 2019, from THERMOPEDIA™: <http://thermopedia.com/content/1211/>
- Bengtson, H. (2019, October 3). *Heat Exchanger Flow: Cross flow, Parallel flow, Counter Flow Heat Exchangers*. Retrieved from Bright Hub Engineering: <https://www.brighthubengineering.com/hvac/62410-heat-exchanger-flow-patterns/>
- Cengel Y. A., Boles M. A. (2014). *Thermodynamics An Engineering Approach Eight Edition in SI Units*. Singapore: McGraw-Hill Education (Asia).
- Cengel, Y. A., & Cimbala, J. M. (2017). *Fluid Mechanics- Fundamentals and Applications*. New York: McGraw-Hill Education.
- Cengel, Y. A., & Ghajar, A. J. (2015). *Heat and Mass Transfer Fundamentals and Applications*. New York: McGraw-Hill Education.
- Chaturvedi, H. (2017, March 15). *What is grid independency test?* Retrieved from Quora: <https://www.quora.com/What-is-the-grid-independent-test>

- Feldmann, D., & Wagner, C. (2012). Direct numerical simulation of fully developed turbulent and oscillatory flows at $Re=1440$. *Journal of Turbulence*, 1-28.
- Feldmann, D., & Wagner, C. (2016). On the influence of computational domain length on turbulence in oscillatory pipe flow. *International Journal of Heat and Fluid Flow*, 229–244.
- Hot Wire Anemometer*. (2019). Retrieved from Circuit Globe: <https://circuitglobe.com/hot-wire-anemometer.html>
- Ilori, O. M., Jaworski, A. J., & Mao, X. (2018). Experimental and Numerical Investigations of Thermal Characteristics of Heat Exchangers in Oscillatory Flow. *Applied Thermal Engineering*, 910-925.
- Incropera, F. P., Dewitt, D. P., Bergman, T. L., & Lavine, A. S. (2007). *Fundamentals of Heat and Mass Transfer, Sixth Edition*. Hoboken: John Wiley & Sons, Inc.
- Jalil, S. M. (2019). Experimental and numerical investigation of axial heat transfer enhancement by oscillatory flows. *International Journal of Thermal Sciences*, 352–364.
- Johnston, J. P. (1976). Internal Flows. *Topics in Applied Physics*, 109-169.
- Kamsanam, W., Mao, X., & Jaworski, A. J. (2015). Development of experimental techniques for measurement of heat. *Experimental Thermal and Fluid Science*, 202-215.
- Mohd Saat, F. A., & Jaworski, A. J. (2017). Numerical Predictions of Early Stage Turbulence in Oscillatory Flow across Parallel-Plate Heat Exchangers of a Thermoacoustic System. *Applied Science*.

- Mohd Saat, F. A., & Jaworski, A. J. (2017). The Effect of Temperature Field on Low Amplitude Oscillatory Flow within a Parallel-Plate Heat Exchanger in a Standing Wave Thermoacoustic System. *Applied Science*.
- Nebauer J. R. A., Blackburn H. M. (2009). Stability of Oscillatory and Pulsatile Pipe Flow. *Seventh International Conference on CFD in the Minerals and Process Industries*.
- Patel, J. J., & Joshi, U. V. (2012). Study of the oscillating flow in the circular tube using CFD. *World Journal of Science and Technology*, 46-49.
- Polezhaev, Y. V. (2011, February 2). *External Flows: Overview*. Retrieved from Thermopedia: <http://www.thermopedia.com/content/751>
- Prabhakara, S., & Deshpande, M. D. (2004). The No-Slip Boundary Condition in Fluid Mechanics.
- Ronquillo R. (2019). *Understanding Heat Exchangers*. Retrieved September 15, 2019, from Thomas for Industry: <https://www.thomasnet.com/articles/process-equipment/understanding-heat-exchangers/>
- Schoenmaker, L. (2017). *Simulations of steady and oscillating flow in diffusers*.
- Shah, R. K., & Sekulic, D. P. (2003). *Fundamentals of Heat Exchanger Design*. Hoboken: John Wiley & Sons, Inc.
- Spakovszky, Z. S. (2019). *Massachusetts Institute of Technology*. Retrieved September 15, 2019, from Thermodynamics and Propulsion: <https://web.mit.edu/16.unified/www/FALL/thermodynamics/notes/node131.html>

Svärd, M. (2014, February 1). *What is the difference between "Grid Independent Test" and "Mesh Convergence Study"?* Retrieved from ResearchGate:
https://www.researchgate.net/post/What_is_the_difference_between_Grid_Independent_Test_and_Mesh_Convergence_Study

www.edsl.net. (n.d.). *EDSL*. Retrieved from EDSL:
<http://www.edsl.myzen.co.uk/downloads/misc/3D%20CFD%20Scaling%20Grid%20Independence%20Test.pdf>

Yoo, S.-Y., Kwon, H.-K., & Kim, J.-H. (2007). A Study on Heat Transfer Characteristics for Staggered. *Journal of Mechanical Science and Technology*, 505-512.



LIST OF APPENDICES

APPENDIX	TITLE	PAGE
A	Gantt Chart FYP I	54
B	Gantt Chart FYP II	55
C	Static pressure monitor for DR 1.2% at location $x_p = 4.5866\text{m}$.	56
D	Velocity at X-axis monitor for DR 1.2% at location $x_p = 4.5866\text{m}$.	57
E	Figure E-1: Data taken from Ansys and tabulated for DR 0.83%	58
	Figure E-2: Data taken from Ansys and tabulated for DR 1.2%	58
	Figure E-3: Data taken from Ansys and tabulated for DR 1.5%	58
	Figure E-4: Data taken from Ansys and tabulated for DR 2.0%	59
F	Figure F-1: Mesh of 50000	60
	Figure F-2: Mesh of 100000	61

APPENDIX A

Table A: Gantt Chart FYP I

Gantt Chart for PSM 1																
Project Activity	Week															
	1	2	3	4	5	6	7	8	9	10	11	12	13	14	15	
Project and Title Selection										Mid Term Exam						
Research on heat exchangers, tube banks, CFD flow simulation, oscillatory flow.																
Chapter 1: Introduction																
a) Background																
b) Problem Statement																
c) Objectives																
d) Scope of the Study																
Chapter 2: Literature Review																
Chapter 3: Methodology																
Submission of Progress Report 1																
Modelling Geometry and Flow Domain																
Establishing the Boundary and Initial Conditions																
Mesh Generation																
Solving and Visualizing																
Report writing																
Final Report Submission																
PSMI Seminar																

APPENDIX B

Table B: Gantt Chart for FPY II

Project Activity	Week														
	1	2	3	4	5	6	7	8	9	10	11	12	13	14	15
Improvement on Literature Review										Mid Term Exam					
Simulation for different DR (1.5% and 2.0%)															
Extraction of results from the simulation (analysis and discussion)															
Writing the Report															
Submission of PSM 2 Report															
Preperation for Slide Presentation															
PSM 2: Panel Presentation															

APPENDIX C

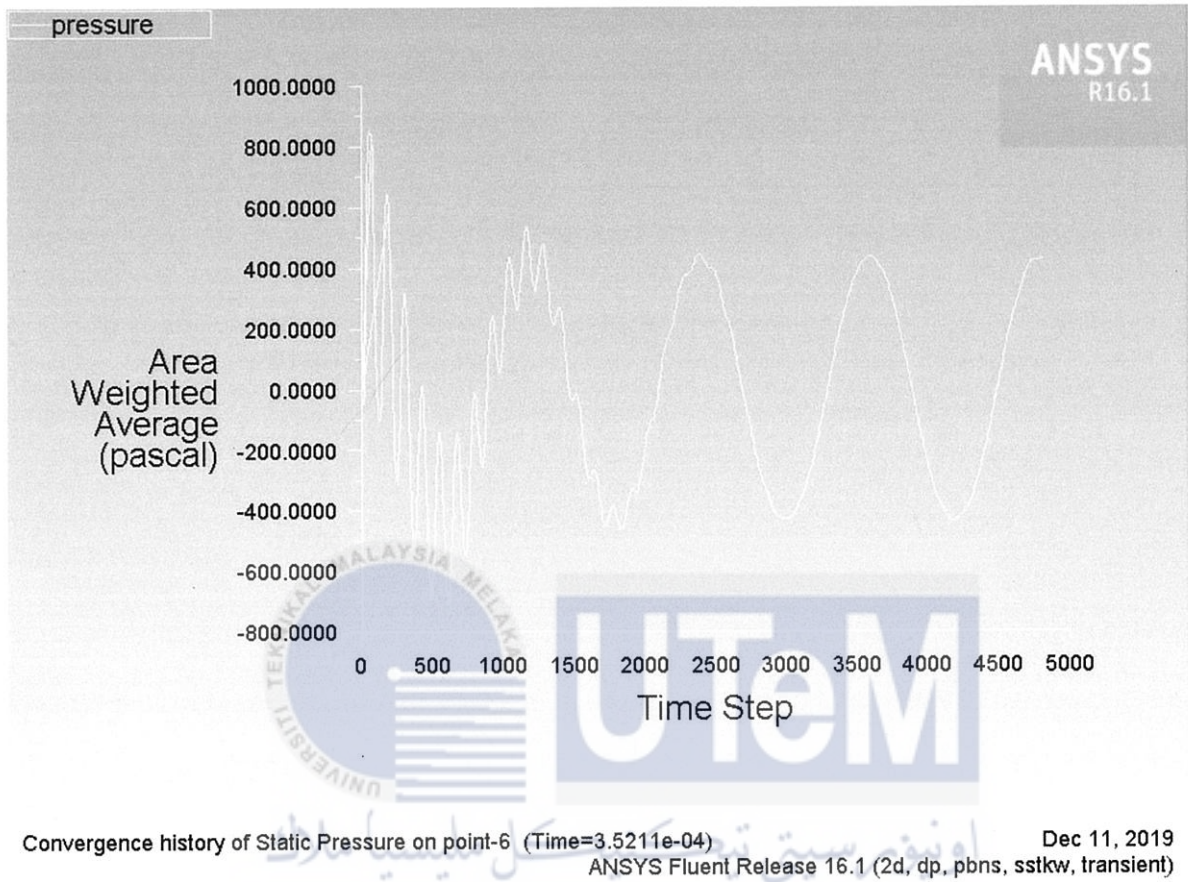
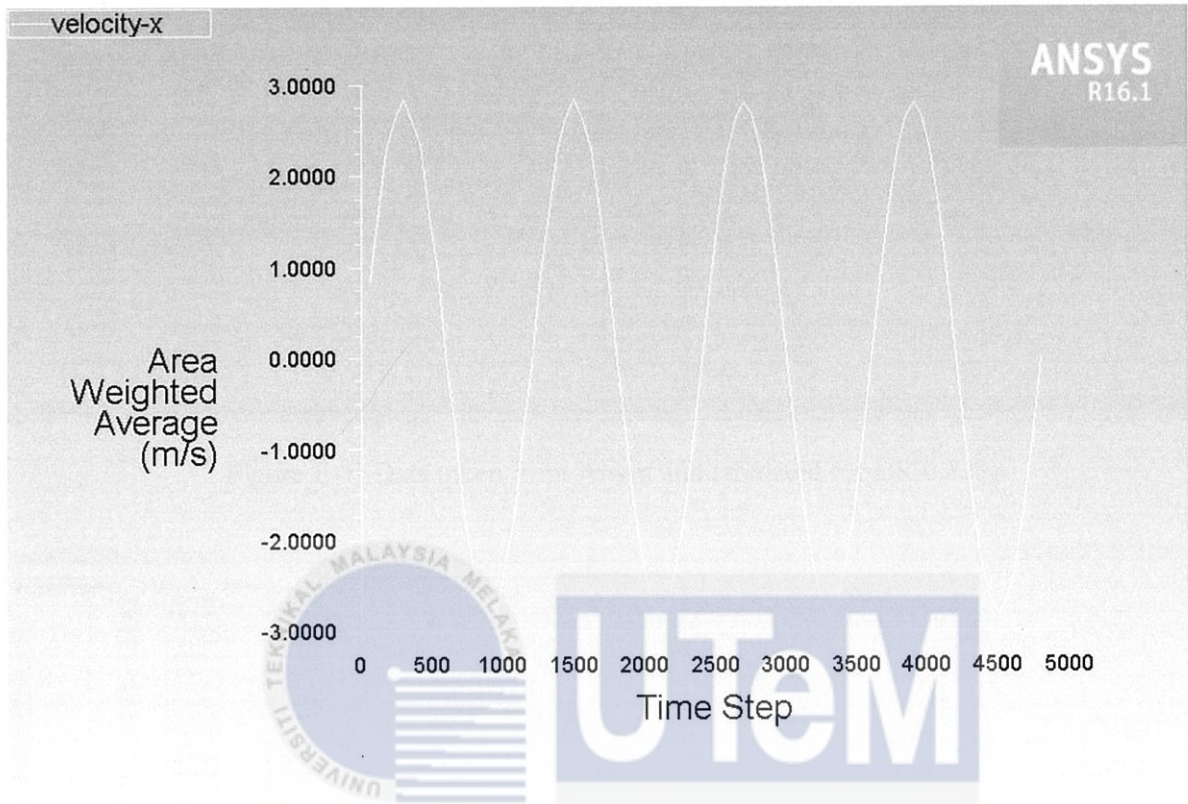


Figure C: Static pressure monitor for DR 1.2% at location $x_p = 4.5866\text{m}$

APPENDIX D



Convergence history of X Velocity on point-6 (Time=3.5211e-03) Dec 11, 2019
ANSYS Fluent Release 16.1 (2d, dp, pbns, sstk, transient)

UNIVERSITI TEKNIKAL MALAYSIA MELAKA
Figure D: Velocity at X-axis monitor for DR 1.2% at location $x_p = 4.5866\text{m}$

APPENDIX E

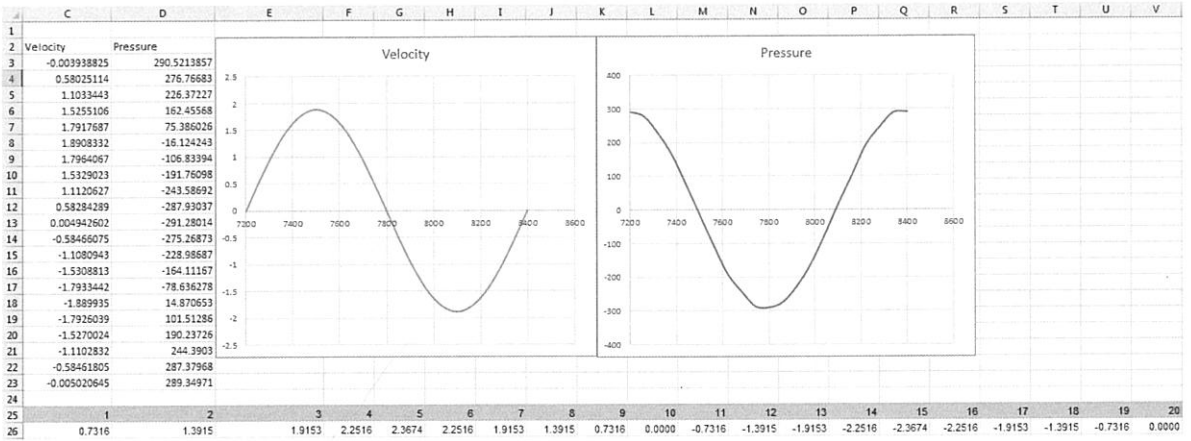


Figure E-1: Data taken from Ansys and tabulated for DR 0.83%

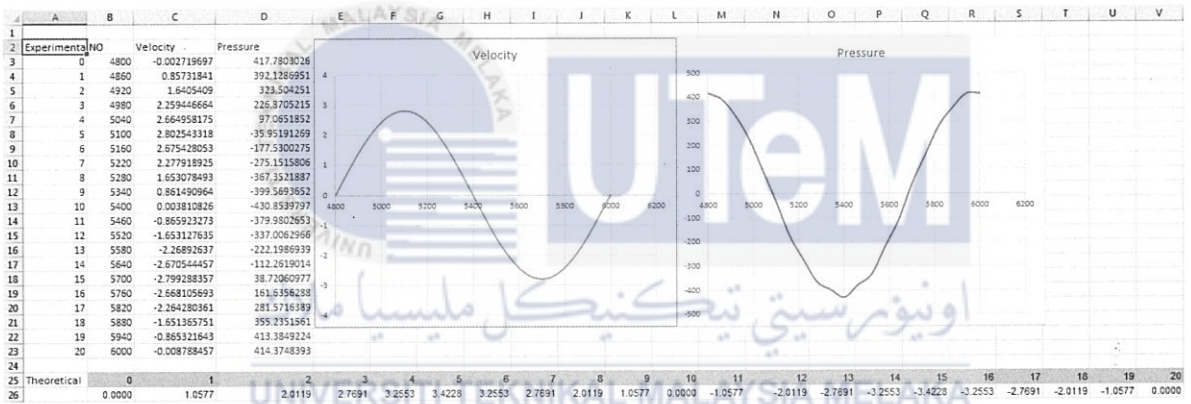
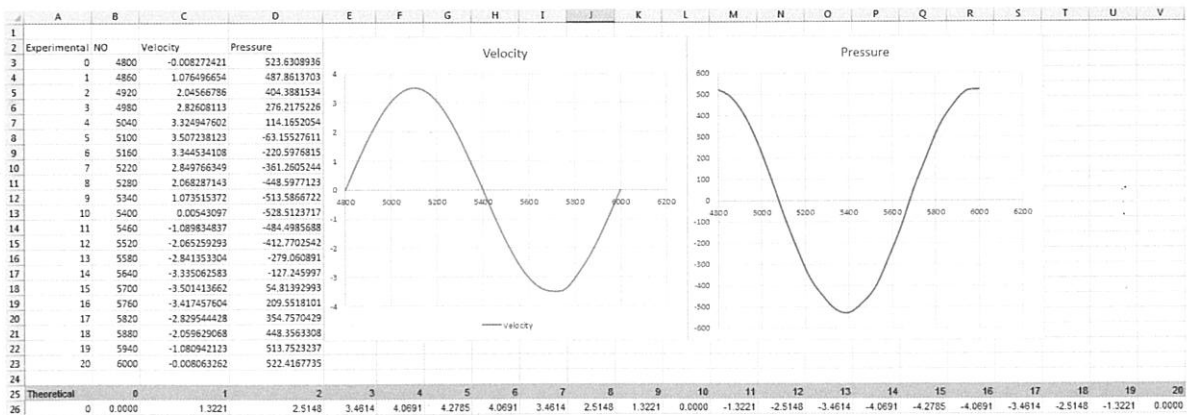


Figure E-2: Data taken from Ansys and tabulated for DR 1.2%



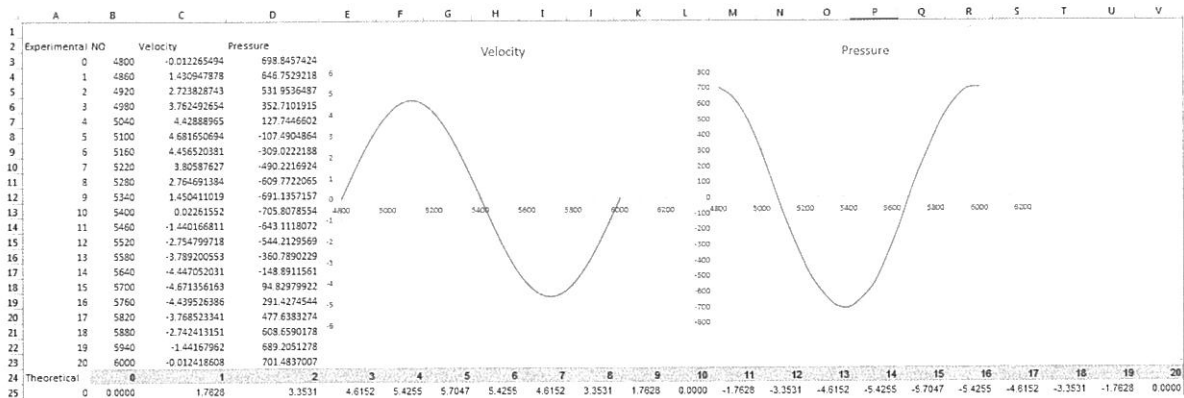


Figure E-4: Data taken from Ansys and tabulated for DR 2.0%



APPENDIX F

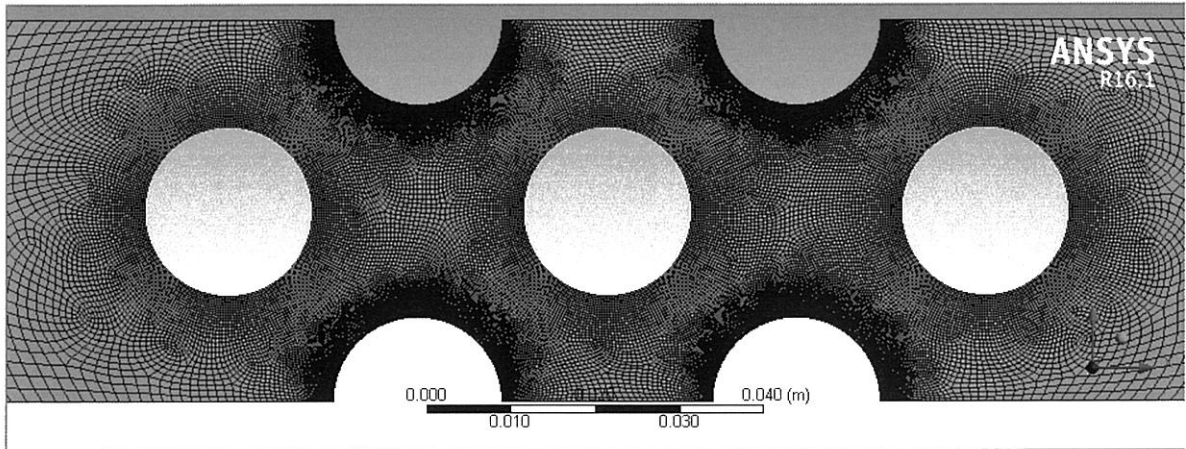


Figure F1: Mesh of 50000

Nodes	52403	Mesh Metric	Aspect Ratio
Elements	51253	Min	1.
Mesh Metric	Skewness	Max	7.9084
Min	9.9589e-006	Average	1.1978
Max	0.57451	Standard Deviation	0.49174
Average	7.9075e-002		
Standard Deviation	9.1051e-002	Mesh Metric	Orthogonal Quality
		Min	0.68407
		Max	1.
		Average	0.98573
		Standard Deviation	2.969e-002

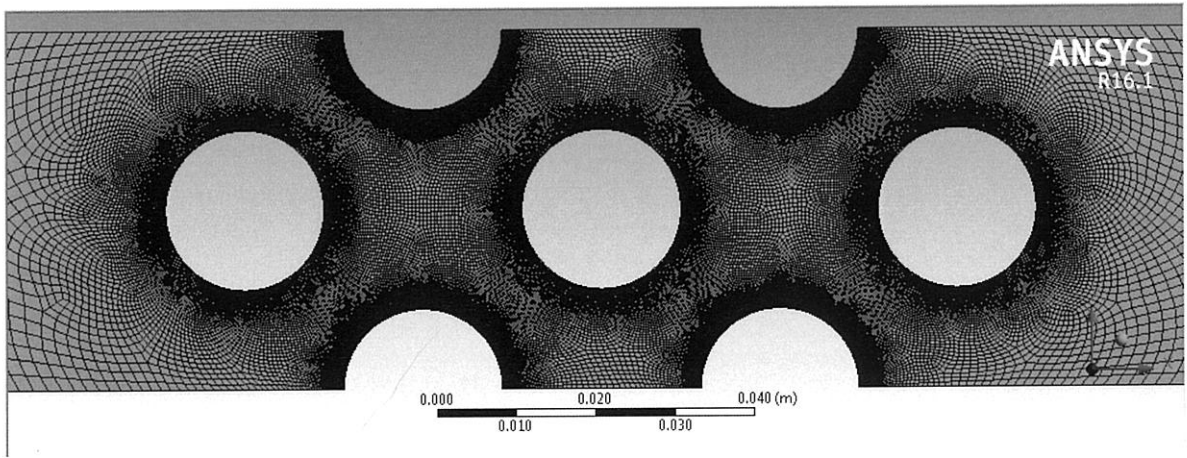


Figure F-2: Mesh of 100000

<input type="checkbox"/> Nodes	100461
<input type="checkbox"/> Elements	98693
Mesh Metric	Skewness
<input type="checkbox"/> Min	5.9818e-006
<input type="checkbox"/> Max	0.65444
<input type="checkbox"/> Average	7.9513e-002
<input type="checkbox"/> Standard Deviation	8.9957e-002

Mesh Metric	Aspect Ratio
<input type="checkbox"/> Min	1.
<input type="checkbox"/> Max	7.8331
<input type="checkbox"/> Average	1.1602
<input type="checkbox"/> Standard Deviation	0.3649

Mesh Metric	Orthogonal Quality
<input checked="" type="checkbox"/> Min	0.57711
<input type="checkbox"/> Max	1.
<input type="checkbox"/> Average	0.98606
<input type="checkbox"/> Standard Deviation	2.9281e-002